View metadata, citation and similar papers at core.ac.uk

brought to you by CORE

provided by Lehigh University: Lehigh Preserve

Lehigh University
Lehigh Preserve

Fritz Laboratory Reports

Civil and Environmental Engineering

1981

User's manual, Bovas-bridge overload analysis - steel (VERSION 1.0), June 1981, 72p.

J. C. Hall

C. N. Kostem

Follow this and additional works at: http://preserve.lehigh.edu/engr-civil-environmental-fritz-lab-reports

Recommended Citation

Hall, J. C. and Kostem, C. N., "User's manual, Bovas-bridge overload analysis - steel (VERSION 1.0), June 1981, 72p." (1981). *Fritz Laboratory Reports.* Paper 2207.
http://preserve.lehigh.edu/engr-civil-environmental-fritz-lab-reports/2207

This Technical Report is brought to you for free and open access by the Civil and Environmental Engineering at Lehigh Preserve. It has been accepted for inclusion in Fritz Laboratory Reports by an authorized administrator of Lehigh Preserve. For more information, please contact preserve@lehigh.edu.

INELASTIC OVERLOAD ANALYSIS OF

STEEL MULTIGIRDER HIGHWAY BRIDGES

FRITZ ENGINEERING
LABORATORY LIBRARY

by

Carl A. Heishman

Celal N. Kostem

Fritz Engineering Laboratory
Department of Civil Engineering
Lehigh University
Bethlehem, Pennsylvania

January 1983

Fritz Engineering Laboratory Report No. 432.7

Parts of this work were sponsored by the Pennsylvania Department of Transportation and the United States Department of Transportation, Federal Highway Administration.

The contents of this report reflect the views of the authors, who are responsible for the accuracy of the data presented herein. The contents do not necessarily reflect the official view or policies of the Pennsylvania Department of Transportation or the Federal Highway Administration. This report does not constitute a standard, specification, or regulation.

TABLE OF CONTENTS

TABLE OF CONTENTS (continued)

TABLE OF CONTENTS (continued)

ABSTRACT

The report presents the application of an inelastic overload analysis to two steel multigirder highway bridges using the finite element method. The previously developed computer program BOVAS (Bridge OVerload Analysis-Steel) was modified from a research to a production oriented tool in phase one of the reported research by simplifying the input-output options. This resulted in two versions of program BOVAS, "detailed" (the original program) and "short" (the new simplified version).

In phase two of the reported research the reliability of the detailed version of program BOVAS was verified by comparisons with available analytical results and laboratory and field overload test results.

A brief description of the analytical method employed and the assumptions made have also been included in the report.

1. INTRODUCTION

1.1 Introduction

This report presents the application of an inelastic overload analysis to steel multi-girder highway bridges by using the finite element method. Hall and Kostem developed and verified a mathematical model which predicts the overload response resulting from the placement of overweight vehicles on simple span or continuous multi-girder highway bridge superstructures with steel I-section girders and a reinforced concrete deck (Refs. 10, 11, and 12). A computer program with the acronym of BOVAS (Bridge Overload Analysis - Steel) was developed in order to solve the mathematical model. This thesis extends the earlier research into a production tool by modifying the program and verifying the new version of the program.

The technique, developed by earlier research, is a computer based analysis scheme employing the finite element method for the analytical modeling of the superstructure. The bridge superstructure is divided into a series of plate and beam finite elements (Fig. 1) which are interconnected at discrete node points (Fig. 2). These finite elements are then further subdivided into layers in order to facilitate the inclusion of material nonlinearities in the analysis (Fig. 3). While the finite element idealization was developed and

successfully applied for previous research of reinforced and prestressed beam bridges (Refs. 23, 24, 31, 33, 34, 39, and 40), it has also been successfully applied in the simulation of the structural response phenomena of steel girder bridges (Refs. 10, 11, and 12).

Inclusion of material nonlinearities necessitates adoption of a particular solution scheme other than that used for linearly elastic problems. Thus the previously developed solution scheme uses a tangent stiffness, or piecewise linear solution process, to simulate the expected inelastic structural response. In this process the loads are applied in a series of load increments or load steps in order to allow for changes in the overall structural stiffness due to nonlinear response. Within each of these load increments iterations may take place so as to ensure convergence of the solution. This tangent stiffness solution process provides a continuous description of the structural response from initial load levels in the elastic range up to the collapse or termination load levels.

The reliability of this technique has been demonstrated for both reinforced and prestressed concrete beam bridges and for steel girder bridges. This thesis, using the modified program, illustrates the reliability of the new model with a few comparisons between experimental and analytical results. Satisfactory agreement was obtained for all test cases. Thus, the modified version of the program has been verified.

1.2 Problem Statement

The overloading of steel girder-reinforced concrete slab highway bridges, hereafter referred to as steel bridges, has become a relatively common occurrence due basically to three factors:

(1) increases in the allowable vehicular weight limitations,

(2) transportation of heavy industrial, military, and construction equipment, and

(3) the issuing of overload permits for specialized overweight and oversized vehicles.

Because of this increased frequency of structural overloads, the bridge engineer has an urgent responsibility to accurately assess the reserve capacity and serviceability limits of any bridge superstructure on which overload vehicles are expected to traverse.

Since an accurate overload analysis requires knowledge of the actual distribution of forces and stresses in the component members, the commonly used reverse design method of analysis is inadequate because the loads are distributed to the girder and slab according to assumed distribution factors. This distribution factor approach cannot be used in the overload analysis for several reasons. First, while the distribution factors are known for the elastic region and at the ultimate limit when all lanes have a uniformly distributed loading, the distribution factors are not known for the transition region between these two bounds where the forces are redistributed as the stiffness of the structure decreases

as damages initiate and progress through the structure. Secondly, the distribution factors have been developed for AASHTO design vehicles and loadings. However, many overload vehicles cannot be considered as AASHTO design vehicles because of unusual axle loadings and spacings. Therefore, some other method besides the distribution factor approach must be used for overload analyses.

Hall and Kostem (Refs. 10, 11, and 12) have developed an acceptable overload analysis for steel bridges. Their method accurately predicts the response of the structure for the expected types of overload vehicles. Furthermore, if during an overload the slab cracks or the girder yields or buckles, their method can predict the following:

(1) the location of any damage to the structure,

(2) the strength of the component after damage, and

(3) the manner in which the forces and stresses will redistribute themselves due to the damage from the elastic region through the ultimate limit.

Such an analysis scheme can permit through the application of known serviceability limits the defining of permissible overloads. For example, if one assumes that 75% of the yield stress is the maximum allowable stress (i.e. serviceability limit) for a given bridge and overload configuration, a computer analysis can be performed. Thus the permissible overload will be the load level which induces stresses of this intensity. This point is illustrated further in Sections 4.2.3 and 4.3.2 of this thesis.

1.3 Purpose and Scope of the Research

The purpose of this research is to transform the computer program developed by Hall and Kostem (Refs. 10, 11, and 12) into a production tool for practical application. Two phases of research are required in order to achieve this goal. The two phases are:

(1) the expansion, modification, and simplification of the computer program which is capable of analyzing the overload response of steel bridges (Refs. 15 and 16), and

(2) the verification of the modified program by the testing of the program.

This report includes the following material:

1. A brief description of the analytical techniques and assumptions employed to model the structure (see Chapter 2).
2. A description of the analytical modeling scheme employed (Chapter 2).
3. A brief description of the modifications to the program accomplished in phase one of this research (Chapter 2).
4. A description of the bridges considered in the verification of the computer program (Chapter 3).
5. Verification of the program through comparisons with actual test results (Chapter 4).

6. Conclusions and other considerations which resulted from the verification of the computer program (Chapter 5).

1.4 Previous Research

The objective of this research is the determination of the overload response of simple span or continuous steel multi-girder highway bridge superstructures. Therefore, only those works which are reported upon in the literature and which are applicable to the present problem will be reviewed. It should be noted that all of this research refers to girders of solid cross-sections and should not be applied to box girders.

Beam-slab highway bridge superstructures can be divided into two categories: those with reinforced or prestressed concrete beams (concrete bridges) and those with steel girders (steel bridges). While many similarities exist when comparing the response characteristics of these two types of bridges, concrete bridges and steel bridges also have many response characteristics which are applicable only to one or the other. For example, a concrete bridge will normally fail due to excessive cracking of the concrete beams, while a steel bridge can fail because of extensive yielding of the girder or because of the buckling of webs or flanges. Thus, those response characteristics which are evident in steel bridges may not occur in concrete bridges and vice versa.

The first developmental work concerning the analysis of structures with concrete decks and steel girders was presented by Newmark in two papers (Refs. 29 and 36). The first of these papers did not consider the composite action of the beam and slab. The second paper overcame this deficiency and presented a derivation for the differential equation describing the axial forces of the component parts in the elastic region. However, this equation was applicable only to isolated T-beams and not to multi-girder systems. Others have expanded upon the theory formulated by Newmark to account for non-uniform connector spacing, initial spacing, initial strains, and nonlinear material properties using an iterative solution procedure.

Proctor, Baldwin, Henry, and Sweeney at the University of Missouri (Ref. 4) and Yam and Chapman at Imperial College (Ref. 43) treat the boundary value problem as an initial value problem and solve the equations by successive approximation; and Dia, Thiruvengadam and Siess at the University of Illinois (Ref. 8), Wu at Lehigh University (Ref. 42) and Fu at the University of Maryland (Ref. 9) use finite differences in conjunction with Newmark's work. None of these methods, however, considers fully the problem of shear lag, shear deformation of the girder, slip between the slab and the girder, and continuous structures; whereas, Tumminelli and Kostem (Ref. 37) employed a finite element method to include the above deficiency into a linear elastic solution process with no inelastic capabilities.

Research by Wegmuller and Kostem (Refs. 39 and 40) led to the development of an analysis technique and computer program to predict the elastic-plastic structural response of eccentrically stiffened plate systems. This technique, which employed the finite element method, used the ACM (Ref. 1) rectangular plate element modified for in-plane displacement by Clough (Ref. 7). The elements were layered to monitor the spread of damage throughout the structure. In addition, the material was assumed to follow the von Mises yield condition. Based on this work Kulicki and Kostem (Refs. 22 and 24) extended the model and technique to incorporate eccentrically placed reinforced concrete or prestressed concrete beams. In this analysis the response characteristics of the concrete beams were realistically modeled, including the cracking and crushing of concrete and yielding of steel. Subsequently, Peterson and Kostem (Refs. 31, 33, and 34) further extended the analysis technique to accurately simulate the biaxial behavior of reinforced concrete slabs, and thus in the end, to reliably predict the overload response of concrete highway bridge superstructures. However, this still left the problem of the overload analysis of steel bridges to be solved.

The above research efforts have demonstrated that the finite element method of analysis provided an efficient tool that can be used to perform an inelastic analysis of eccentrically stiffened slab systems. The complexities in material behavior and losses in stiffness due to yielding, cracking, crushing, or local instability can be directly incorporated into the analysis scheme. Thus, by

integrating the works by Tumminelli and Kostem and Peterson and Kostem, and including the effects of strain hardening, flange buckling, and web buckling into a concise finite element computer program, a realistic model for predicting the overload response of continuous steel multi-girder highway bridges was developed by Hall and Kostem (Refs. 10, 11, and 12).

2. ANALYTICAL MODEL

2.1 Introduction

The analytical model should adequately reflect the structural characteristics of the actual structure. To reliably describe the inelastic response of beam-slab highway bridge superstructures with steel girders and a reinforced concrete deck slab, the following phenomena must be considered:

(1) The out-of-plane or flexural behavior of the structure.

(2) The in-plane response of the girders and slab due to eccentricity of the girders.

(3) The coupling action of the in-plane and out-of-plane responses.

(4) Material nonlinearities.

(5) The possibility of slip between the girders and the slab (i.e. amount of composite action).

(6) Shear deformation of the girders.

(7) Local instability of the girder and/or girder flanges or webs, and any associated post-buckling behavior.

When bridge superstructures are subjected to vehicular loads, both out-of-plane responses due to the longitudinal and transverse bending moments and in-plane responses resulting from the axial forces occur in the slab. At the same time, longitudinal bending moments and axial forces are predominant in the girders. These axial forces develop in the slab and girders because of the eccentricity of the reference plane of the girders relative to the reference plane (midheight) of the slab. Thus, the application of out-of-plane loads to the bridge superstructure produces both in-plane and out-of-plane responses in the slab and girders. This interdependency between in-plane and out-of-plane actions is commonly referred to as coupling action. While coupling action has little effect on the structural response in the elastic region, it does have a significant effect on the inelastic or nonlinear structural response as explained in detail in Ref. 34.

Since the response due to overloading is expected to eventually cause nonlinear stress-strain behavior, the appropriate stress-strain relationships of the component materials must be included. Thus, the present analysis scheme as developed by Hall and Kostem (Refs. 10, 11, and 12) utilizes the biaxial stress-strain relationships developed in Refs. 25, 26, 27, 28, 31, and 34 to describe the inelastic behavior of concrete slabs, and in addition, utilizes the uniaxial stress-strain relations developed in Refs. 10, 11, 19, 22, 23, and 35 to describe the inelastic response of steel.

To account for the variation of material properties through the depth of the slab and the girders, the finite elements are subdivided into a series of layers (Fig. 3). Each layer is assumed to have its own distinct material properties and is also assumed to be either in a state of uniaxial or biaxial stress. Thus, the progression of nonlinear material behavior through the structure can be monitored by defining the stress-strain relationship on a layer by layer basis. Through the utilization of the layering technique, good agreement has been obtained between analytical and test results (Refs. 5, 13, 14, 22, 24, 32, 38, and 41).

Typical analytical models for composite structures assume that no slip occurs between the slab and the girders. However, if sufficient linkage does not exist between the slab and the girders, then slip will occur and the percentage of load shared by the slab and the girder will change. The analytical model should be able to account for the possibility of slip. In addition to slippage, the model should be able to adequately reflect the effects of shear deformation since girders and particularly plate girders with thin webs will deflect considerably more than standard beam theory would predict. Finally, because beams and plate girders are of thin walled open cross-sections, they are susceptible to local buckling phenomena prior to attaining maximum stress conditions. Thus, the analytical technique should be capable of predicting the occurrence of local buckling and any post-buckling strength of such sections.

The preceding paragraphs have presented the major structural phenomena that have a significant effect on the behavior of steel bridge superstructures. The underlying premise of the entire nonlinear analysis is that the primary response of the structure is flexural in nature with the in-plane and coupling actions and that the ultimate collapse of the bridge superstructure is a result of flexural failure or local instability (i.e. buckling).

Structural phenomena considered to be of secondary importance and excluded from the analysis technique are minor axis bending of the girders, shear punch failure of the slab, torsional stiffness of the girders, and superelevation.

2.2 Model Assumptions

Only the assumptions pertinent to the specific features of the analysis are presented in this thesis. A detailed treatment of the finite element method as applied to this research is presented in a number of other related reports (Refs. 10, 12, 22, 24, 31, 33, and 37).

The following assumptions are made with regards to the development of the analytical model. The analytical model and associated computer program is capable of analyzing steel bridges having the following characteristics:

(1) The bridge can be of simple span or continuous construction.

(2) While full composite interaction between the deck slab and the girders is usually assumed, non-composite or partial composite interaction can also be assumed. However, the reliability of the results is not guaranteed, if the user assumes slip exists between the girders and the slab.

(3) The bridge deck must be a monolithic reinforced concrete slab.

(4) Steel beams or girders of varying or constant cross-section may be considered.

(5) Girder spacing(s) must be constant for a given bridge.

(6) While the diaphragms and cross-bracing contribute to the structural stiffness of the superstructure, their contribution to the stiffness can be neglected for the type of loadings considered.

(7) It is assumed that the effects of the vertical and longitudinal stiffeners are local and therefore they can be neglected in the overall structural behavior. However, the effects of the vertical stiffeners are included in the shear panel buckling analysis.

(8) It is assumed that the bridge girders may deform in shear and major axis bending.

(9) The stresses in the slab are due to the biaxial bending of the slab and the axial forces that may develop in the deck slab in the longitudinal and transversal directions.

(10) The bridge superstructures to be analyzed are limited essentially to right bridges (i.e. a skew angle of 90^{o}). However, previous research (Refs. 21 and 34) has indicated that bridges with moderate skews down to 60^{o} can be analyzed with little loss in accuracy.

(11) Plane sections remain plane before and after deformation of the slab and girder except that a Timoshenko approach has been used to include shearing deformation in the girder.

(12) Because the deformations are assumed small in comparison to the dimensions of the slab and girder, the model assumes that the girders and slab do not change thickness. It should be noted that previous experience with bridge overloading (Ref. 33) supports this assumption.

(13) Small strains are assumed. Thus, first order linear strain-displacement relationships can be employed. (Ref. 33).

(14) The plate and beam finite elements are layered, each layer having its own stiffness properties,

so as to accurately model material nonlinearities and progressive material failure.

(15) When the average stress of all the compression flange layers of any beam element exceeds the critical buckling stress, the compression flange is assumed to buckle. In order to model the post-buckling strength, layers which exceed the critical buckling stress are assigned low stiffness values. Similarly, when the average stress state of the web plate panel reaches the critical stress (buckling stress) all of the web layers of the entire web plate panel are assigned lower stiffness values.

(16) An impact factor is applied by the model to the actual "vehicle" loading. The impact factor for simple spans is calculated in accordance with Ref. 3, while the impact factor for continuous structures uses the same formula except that the length is assumed to be an average span length.

(17) Other less important assumptions can be found in other related reports (Refs. 10, 11, 12, and 15).

2.3 Solution Scheme

The developed solution scheme solves the overload problem in a logical sequence of operations. The solution process consists of four main phases:

(1) Problem Definition

(2) Dead Load Solution

(3) Scaling Procedure

(4) Overload Solution Procedure

A simplified logical flow chart of the sequence of operations for program BOVAS is shown in Fig. 4. More detailed descriptions of the four main phases are presented in the following sections.

2.3.1 Problem Definition

This phase defines the particular problem that will be solved. To define the problem, two groups of information are required to be input into the program. They are:

(1) Bridge Description

(2) Bridge Loadings

The amount of information required to define the bridge is structure dependent. References 15 and 16 explains in detail the specific information required as input in order for the program to solve the given problem.

In order to fully describe the bridge superstructure the following information must be provided:

(1) Bridge superstructure geometry

(2) Finite element discretization and type of symmetry

(3) Slab description and material properties

(4) Girder description and material properties by layers

(5) Location of any web plate panels

(6) Location and type of any fatigue details

The bridge loadings are composed of three parts:

(1) Dead loads acting on the girders - the dead weight of the "wet" concrete deck, steel girders, and any steel coverplates.

(2) Dead loads acting on the composite superstructure - the dead weight of any curbs, parapets, and future wearing surface

(3) Live load or overload "vehicle" - the truck, dolly, and/or lane loading to be investigated by the program.

In order to define the loading, the magnitude or intensity of the loads and the position of all loads must be provided. The live load is typically positioned such that a worst case analysis results. All loads should be defined as static loads, but the program will amplify the live load by an impact factor as described in Section 2 .2 of Chapter 2.

2.3.2 Dead Load Solution

Since the analytical modeling scheme presented in the report considers material nonlinearities, which are stress dependent, an accurate assessment of the stress state prior to the application of the overload is required. Because of the possible nonlinear behavior of the structure, the principle of superposition cannot be employed. Therefore, prior to the application of the overload the superstructure must be analyzed to obtain the stresses in the slab and girders due to the two components of the dead load discussed in Section 2.3.1. The initial stress state and any material failures or nonlinearities due to the application of these dead loads will thus be reflected prior to the application of the overload.

2.3.3 Scaling Procedure

As long as the initial solution due to the overload produces a linearly elastic response, the load is increased proportionally to the lowest load level corresponding to one of the following element stress limitations:

(1) 60% of the compressive strength of concrete,

(2) 90% of the tensile strength of concrete,

(3) 97.5% of the yield strength of the steel, or

(4) 100% of the buckling stress.

Because this technique scales up the initial load level, only one elastic solution is obtained. Thus, the number of elastic solutions are kept to a minimum. All subsequent solutions will exhibit nonlinear response.

However, if the initial solution causes any material or stability failure, the initial live load is scaled down in order that a linear elastic solution can be obtained. Then the scaled down load is incremented until nonlinear response occurs. Once nonlinear response begins, the overload solution is employed.

2.3.4 Overload Solution

The overload solution is solved using a tangent stiffness approach (a piecewise linearization of the nonlinear phenomena). In such an approach the system of equations is assumed to be linear in a given load increment. By computing the tangent to the stress-strain curve for each layer based upon the current stress state, the layer stiffnesses, element stiffness, and ultimately the global stiffness matrix is calculated. After calculating the nodal point displacements and element layer strains for the load increment, the corresponding element layer stresses are obtained by the program for the load increment by employing the material stress-strain relationships. These incremental stress values are added to the total stress state which existed prior to the application of the load increment, thus arriving at a new current stress state. The process is repeated (iterated) with the new current stress state until the solution for the increment converges. If a layer fails during the application of the load increment, the load increment is scaled down so that the layer stress causes incipient failure. Thus, in this method which is called the "incremental-iterative" method, the stiffness matrices are continually updated within each

load increment or step. It should be noted that the initial solution of each load cycle is based upon zero stress and displacement increment values; thus, the first iteration of each load step is based upon the stiffness matrix of the previous load cycle. The overload analysis process terminates when one of the specified termination checks is exceeded.

Allowable limits on deflections; live loads; stresses; strains; number of cracked, crushed, or yielded layers; and crack widths can be specified for the deck slab and/or girders to define the serviceability limits of the bridge superstructure (Refs. 15 and 16). These checks are used to terminate the overload solution procedure if any one of the specific serviceability limits is exceeded.

2.4 Modifications to the Original Program

The computer program developed by Hall and Kostem was extensively modified in phase one of this research work. Two separate programs evolved from the original program. The first version, hereafter referred to as the detailed version, was developed during the thesis work and is verified by this thesis. The second version, hereafter referred to as the simplified version, was also developed during this thesis, but this version has not been verified.

The major emphasis in the development of the two programs was placed on the reduction of the input to the original program. Many former input values are now internally defined within the program or internally calculated during the execution of the program. The user no longer has to input the discretization, the boundary conditions, the slab layering, or as many material properties in the detailed version. Furthermore, in the simplified version the girder layering and dead loads are also internally calculated. Approximately eighty input variables were removed from the original version of the program in the development of the detailed version. The simplified version was developed by removing approximately twenty-five additional input variables from the original program. Many of these variables were arrays which were read several times within one analysis.

To illustrate the reduction of input to the program, a comparison between the original, detailed, and simplified versions is made for the two test bridges presented in Chapter 3. For the first example bridge presented in Chapter 3, the original program required approximately 120 cards with nearly 400 input entries. The detailed version reduced the input to 53 cards with approximately 150 input entries, while the simplified version only requires about 15 cards with approximately 30 input entries. A substantial reduction in input is also evident for the second example bridge (see Chapter 3) when comparing the three programs. The original program required 112 cards and 314 input entries. While the detailed

version reduced the input to 42 cards and nearly 125 input entries, the simplified version requires only 20 cards and approximately 60 entries.

The simplified and detailed versions of the program can be effectively used in a production environment because of the reduced input. The detailed version which has greater flexibility in the input of the program than the simplified version is recommended only for unusual bridges. For example, bridges with unusual hybrid construction, with haunched girders, or with severe deterioration should be modeled only by the detailed version. For other bridges, the simplified version should provide acceptable results. A complete description of the two programs, the input for each program, and the preset control parameters to each program can be found in Refs. 15 and 16.

3. TEST BRIDGES

3.1 Introduction

In order to verify the modified computer program, comparisons must be made between analytically produced results and data obtained from experimental testing. This chapter will describe the bridge superstructures and loadings used for the verification of the detailed program, while the next chapter will present the results of the comparison. Two full scale concrete slab and steel girder structures, which were previously subjected to overload testing and reported on in the available literature were analyzed by the non-linear finite element method.

3.2 Example Bridge 1 - AASHTO Bridge 3B

The first example bridge is the AASHTO (formerly known as AASHO) Bridge 3B which was constructed as part of the AASHTO Road Test conducted in the early 1960's (Refs. 17 and 18). Bridge 3B was designed as a simply supported fully composite reinforced concrete slab and steel girder bridge with a span length of 15.24 m (50 ft.) centerline-to-centerline of bearing. The concrete deck slab for the bridge had an average measured depth of 164 mm (6.45 in.) and was 4.57 m (15 ft.) wide. Three W18X60 steel girders were placed 1.52 m (5 ft.) apart with 11.1 mm x 152 mm (7/16" x 6") coverplates

extending over 5.64 m (18.5 ft.) of the middle of the span. Figures 5 and 6 show the elevational and cross-sectional views of Bridge 3B.

The loads were applied to the superstructure during the test by moving overload vehicles. For the testing of Bridge 3B three different overload vehicles were used (vehicles 97, 98, and 99 as shown in Fig. 7.). The loading procedure consisted of a truck with constant weight traveling across the bridge usually thirty times. The load on the truck would then be increased and the process repeated. During the loading process the midspan deflections of each girder were monitored and recorded. This procedure continued until the bridge collapsed onto the safety crib below the bridge superstructure.

Since the overload vehicle moved over the bridge, an infinite number of static load configurations were applied to the superstructure. In the general case the slab may be subjected to both longitudinal and transverse bending while the girders are primarily subjected to longitudinal bending. Construction of a static load configuration to simulate the moment envelope and thus to obtain the maximum possible state of stress at every point in both the slab and the girders is very difficult to achieve. Therefore, two different approaches are considered (Ref. 34).

For this particular bridge and loading, the first option is to simulate the overload vehicle as a line load over each girder in the finite element model. The loads should be over the girders for this example since the bridge width and vehicle widths are

approximately the same. Since this idealized load configuration approximates the moment envelope for the longitudinal direction only, the loading will produce primarily longitudinal bending in both the slab and the girders. This moment envelope is produced as the vehicle traverses the superstructure and contains the maximum moment values.

The second option is to simulate the overload vehicle as a rectangular area load. The area load should be selected such that the analysis is equivalent to the maximum static moment diagram produced by the moving overload vehicle. In this idealized loading configuration the slab is subjected to both longitudinal and some transverse bending, while the girders are primarily subjected to longitudinal bending.

A comparison of the two methods in limited testing shows the results of the two approaches are nearly identical for the loads and stresses in the girders. However, the slab behavior is different. The first option does not allow "dishing" of the slab. while the second option allows the slab to "dish". Since the major difference in the two methods is the behavior of the slab and some "dishing" might be expected, the second option is used to simulate the overload vehicle. For this example, the overload has been entered as one rectangular area load at the midspan of the structure.

Meanwhile, the loads included in the dead load on the beam solution are the steel girders and coverplates and the wet concrete

deck. Also only the wooden curbs on each free edge are considered for the dead load on the composite superstructure.

In order to make both the geometry and loadings symmetric with respect to a longitudinal axis of symmetry at the bridge centerline, both overhangs are considered to be 0.91 m (3 ft.) in width. This increases the bridge width from 4.57 m (15 ft.) to 4.87 m (16 ft.) for the full structure. Since the structure is already symmetric about the bridge midspan (transverse axis of symmetry), the bridge could be modeled with quarter, half-longitudinal, half-transverse, or full symmetry. This report will examine three of the four options and compare the results of the three analyses in the next chapter. All symmetry options except half-longitudinal will be considered for this structure.

3.2.1 Quarter Symmetry

Figure 8 shows the superstructure discretized into a series of finite elements for the quarter symmetry option. The load location and element dimensions are indicated in the figure. A total of eighteen slab or plate elements and twelve beam elements were used. It should be noted that because a line of symmetry lies along the axis of the interior girder only one-half of the interior girder cross-section is included in the finite element model.

The layered slab and girder models are shown in Fig. 9. A total of six layers of concrete and four layers of steel reinforcement were used in the slab finite element. The direction of action of the reinforcement is indicated by the cross-hatched area and is

given along with the thickness, bar size, and spacing in Table 1. The beam finite element consists of a total of ten layers as indicated in Fig. 9. The cross-hatched layer, which represents the bottom coverplate, has two sets of material properties. In the region where no coverplate exists in the actual structure (near the supports), the material stiffness properties are set to articically low values to simulate the absence of the coverplate. In the area where there is a coverplate (near midspan), the properties of the steel were used. Table 2 lists the material properties of the girder steel, steel reinforcement, and concrete used in Bridge 3B and the corresponding material properties used in the finite element simulation of the structure. Differences exist between the two sets of data because the program now internally defines many of the material properties which could be input previously.

3.2.2 Half-Transverse Symmetry

Figure 10 shows the superstructure discretized into a series of finite elements for the half-transverse symmetry option. The element dimensions and load location are indicated in the figure. A total of thirty-six slab or plate elements and eighteen beam elements were used. Girder and slab layering as well as material properties are the same for this model as those presented for the quarter symmetry option.

3.2.3 Full Symmetry

The discretization of Bridge 3B for the full symmetry option is presented in Fig. 11. The load location and element

dimensions are indicated in the figure. A total of seventy-two plate elements and thirty-six beam elements were used. Girder and slab layering as well as material properties are the same for this model as those presented for the quarter symmetry option.

3.3 Example Bridge 2 - University of Tennessee Bridge 1

This bridge was one of four bridges which were to be inundated as part of a reservoir in Tennessee (Ref. 6). Bridge 1, referred to as such by the experimental researchers, was a four-span continuous composite structure with span lengths of 21.34 m, 27.43 m, 27.43 m, and 21.34 m (70', 90', 90', and 70'). The bridge was constructed in 1963 and designed for HS20 loading. The deck slab was 178 mm (7") deep and was 10.52 m (34.5') wide including the curb (Fig. 12). For the finite element analysis the curb portion of the superstructure was considered to be in the same plane and of the same thickness as the slab. Four W36X170 steel girders were used to support the deck with a girder spacing of 2.54 m (8.33') centerline-to-centerline between girders. In the negative moment regions there were four W36X160 steel girders with 267 mm x 25.4 mm (10-1/2" x 1") coverplates. A plan view of the superstructure and the location of the applied loads are shown in Fig. 13.

The loads were applied to the bridge deck by eight 890 kN (200 kips) center hole jacks resting on bearing grills. The bearing grills were constructed from two W14X30 steel beams 1.17 m (46") long and 0.76 m (30") center-to-center which were resting on concrete

pads poured directly on the bridge deck. The location of the grills is shown in Fig. 13 by cross-hatched areas.

Due to the symmetry of the structure and the loading about the bridge centerline, only one-half (half-longitudinal) of the structure needs to be modeled. The discretization of the bridge is given in Fig. 14 with the load locations and element dimensions. The cross-hatched areas represent the location of the patch loads that must be applied to the idealized structure. A total of fifty-six slab elements and twenty-eight beam elements were used. The area of main structural interest was the portion of the bridge near the midspan of the loaded span; therefore, the element discretization is finer in this region and much coarser in other spans. While the coarse discretization of the unloaded spans will be sufficient to model accurately the stiffness of the bridge, deflections and stresses in these regions will not be reliable because of the element size and aspect ratio.

The layered slab and beam finite element elements are shown in Fig. 15. A total of six layers of concrete and four layers of steel reinforcement were used. The direction of action of the slab reinforcement is perpendicular to the cross-hatched area and is specified along with the thickness, bar size, and spacing in Table 3. The exact reinforcement and pattern were not given in Ref. 6 so a reinforcement distribution based upon the existing design practices was chosen (Ref. 30). The beam finite element consists of ten layers as indicated in Fig. 15. Because the length of the coverplated

sections were not specified in Ref. 6, the W36X170 girder was used throughout the bridge. Finally, the material properties and parameters assumed for the finite element analysis are listed in Table 4.

4. COMPARISONS OF ANALYTICAL AND EXPERIMENTAL RESULTS

4.1 Introduction

In order to verify the detailed version of the computer program (Ref. 15), comparisons must be made between experimental and analytical results. Several bridge superstructures have been tested with satisfactory agreement in the comparisons made. This chapter will report the results of the comparisons for the two girder-slab bridges described in Chapter 3.

Three types of comparison will be made for the first example bridge. First, a comparison of the analytical results will be made with the reported experimental results (Ref. 18). Secondly, comparisons between the three symmetry options will be made in order to check that the three models give identical results. Finally, comparisons will be made between computer analyses, which terminated at the allowable AASHTO provisions (Refs. 2 and 3) and those which were allowed to approach but not reach the ultimate load of the structure.

The second example bridge was modeled only with half-longitudinal symmetry. Therefore, only the first and third types of comparison mentioned for example bridge one will be made for the continuous span. The experimental results of the second example bridge are given in Ref. 6.

4.2. Example Bridge 1 - AASHTO Bridge 3B

4.2.1 Comparison of Analytical and Experimental Results

In order to compute the analytical and experimental results for the first example bridge, the load-deflection curve and dead load stresses were found in Ref. 18 and compiled in Table 5 along with the analytical results of the full symmetry. The next section will show that the results of the three symmetry options differed by no more than 1%. Therefore if a valid comparison exists between the experimental and full symmetry results, the comparison can also be extended to the quarter and half-transverse symmetry options.

First, in comparing the load-deflection results with the curve found in Ref. 18, the analytical results showed higher deflections than those predicted by the curve. For the 75% of yield stress load, the deflection predicted by the program is nearly 35% higher than experimental results. At higher load levels, the deflections show even more discrepancy. However, some difference between test results and computed results is to be expected, because the loads were applied to the test structure by three different overload vehicles in motion and the finite element program applied an approximate equivalent static loading pattern in an incremental manner. Because the overload was applied as a rectangular area load at midspan instead of a line load as suggested in Ref. 34, the discrepancy is probably compounded. While the discrepancy in deflections is significant, it is believed that modeling the overload as a line load instead of a rectangular area

load would improve the comparison of deflections to within acceptable limits.

Other comparisons yielded favorable results. For example, stresses were reported in Ref. 18 for the two components of the dead load solution (see Table 5). For both solutions, the reported results were higher than the stresses predicted by the program. In the dead load on the beam solution, there is a difference of 6.8% for the exterior girder and 3.0% for the interior girder. The analytical model only considered the dead weight of the steel girders, coverplates, and the "wet" concrete slab, while the experimental results also included the weight of the shear connectors and diaphragms. Also, the actual unit weight of the concrete deck slab had to be assumed for the finite element model since it was unknown. If the assumed unit weight of concrete was less than the actual unit weight, the comparison would be even more favorable. Similarly, the dead load on the structure solution was assumed to only include a wooden curb for the analytical model. However, Ref. 19 indicates additional dead loads were included on the actual structure. They were the weight of the concrete slab extending beyond the supports and the stresses left in the girders because of the weight of the forms. Considering the additional loads on the actual structure for the two dead load solutions, the comparison of stresses between experimental and analytical results is very favorable.

Finally, the progression of failure due to the increasing load is in good agreement. The damages began as yielding of the

bottom flange at the end of the coverplate. Yielding progressed along the end of the coverplate and initiated at the midspan and into the web and coverplate layers, before cracking of the deck began. Cracking of the deck was limited to the bottom layers of the slab initially before progressing through the middle concrete layers.

While there is some discrepancy in the comparison of the analytical and experimental results, they can be justified by the assumptions made in the finite element model. Improving the assumptions will also improve the comparison of results.

4.2.2 Comparison of Symmetry Options

As described in Chapter 3, this bridge was analyzed for quarter, half-transverse, and full symmetry in order to check that identical results were reported by the three analyses. All three models were made with identical discretizations, material properties, loadings, and all other input data. The three symmetries were analyzed until at least one steel girder layer exceeded 75% of the yield stress for that material layer and until the allowable crack width was exceeded in the concrete slab. This permitted the thesis to check the allowable load in accordance with the AASHTO provisions (Ref. 2) and a more extreme but not ultimate load. Tables 6 and 7 present the results of the three computer analyses terminating at 75% of the yield stress (the lower termination check) while Tables 8 and 9 list the results of the other three computer analyses which terminate because the maximum crack width (the higher termination

check) is exceeded. In order to make the comparisons easier to understand, all four tables are presented as if the results of the quarter and half-transverse symmetries were full symmetries.

Looking at Tables 6 and 7, the results can be considered identical for all comparisons and all symmetries. There are two or three comparisons where a very slight difference exists in the third significant figure of the results. This corresponds to a difference of less than 1%. Therefore, these comparisons are valid for loads, deflections, damage levels, and stresses.

Similarly, looking at Tables 8 and 9, the results of the three symmetries are in good agreement. Identical results are shown for the two dead load solutions. However, the overload solution shows slightly different results for each of the three symmetries. All three analyses terminated at load levels within 1% of each other. This slight difference in termination load can be expected to produce differences in the results of the stresses and deflections for the three symmetries. However, even when comparing slightly different load levels, the maximum difference in stresses and deflections only approaches 3%.

4.2.3 Comparison of Two Termination Options

Two termination options were analyzed for each of the three symmetries of example bridge one. The first termination check was activated if at least one steel girder layer exceeded 75% of the yield stress for that material layer. This termination check is in accordance with the AASHTO provisions (Ref. 2). The second

termination check allowed the structure to receive extensive damages but not reach the ultimate load. For the second termination check, if the maximum crack width of 0.1015 mm (0.004") was exceeded, the analysis terminated. This comparison will consider only the results of the full symmetry option since all symmetries have been shown to produce "identical" results.

Table 6 shows the maximum allowable load level permitted on Bridge 3B for the lower termination check. While the bridge was designed for an HS20 truck (324 kN or 72 kips), the program only permits a maximum allowable load of 287.8 kN (64.7 kips) when the impact factor is included in the analysis. However, if the loading is done under controlled conditions (truck moves at crawl speed with escort vehicle), the impact factor can be ignored and the allowable load increases to 370.1 kN (83.2 kips). These computer results appear conservative when compared to the design loading. However, Ref. 18 (page 188) showed the actual stresses exceeded the design stresses by approximately 7% during the experimental testing. Therefore, it appears that the bridge was slightly underdesigned and the program accurately predicts the structural response.

Because the bridge is still in a linearly elastic response region, the lower termination check seems to be overly conservative and impractical for a serviceability limit. Therefore, a second termination check was analyzed in order to achieve nonlinear response and some damage to the structure. Table 8 shows the maximum loads for Bridge 3B when the crack width of 0.1015 mm (0.004") [illegible]

(0.004") is the controlling termination parameter. Because of the excessive damage at this load level, this termination check is not a practical serviceability limit. However, a practical load level can be determined from reducing the data from the program. For example, if the unknown residual stresses can be assumed negligible for this specific bridge, the user may determine that the first yield of the girder is the serviceability limit. In this case in a controlled overload the practical limit becomes 596.1 kN (133.9 kips). For an uncontrolled overload at first yield, the load reduces to 463.5 kN (104.2 kips).

This thesis does not try to suggest a new AASHTO provision for the serviceability of bridges, but does try to show that a higher termination check than the 75% of yield stress should be considered in some cases. If the residual stresses cannot be neglected in the analysis, then the 75% of yield stress is probably an acceptable serviceability limit. However, if residual stresses are less than 25% of the yield stress, higher load levels than those predicted by using the 75% of yield stress limit could be permitted.

4.3 Example Bridge 2 - University of Tennessee Bridge 1

4.3.1 Comparison of Analytical and Experimental Results

In order to compare the analytical and experimental results for the second example bridge, the load-deflection curve and limited qualitative damages were found in Ref. 6 and compiled in Table 10 along with the analytical results. Further comparisons cannot be

made since the experimental results were not reported in more detail.

First, in comparing the load-deflection results shown in Table 10, good agreement is found along the centerline of the bridge and along the exterior girder for the loads shown. The largest discrepancy between the experimental and analytical results is 6.3%. The other three comparisons are different by approximately 2% each.

The first yield load for the second example bridge was reported in Ref. 12 to be 2757.9 kN (620 kips). The analytical model predicted first yield of the girder to occur at 3100.0 kN (696.9 kips). The higher yield load can be explained by the fact that a higher yield steel material was input in order to balance the lack of a coverplate in the model. The higher yield steel material without the coverplate simulated the actual girder with a coverplate. Bearing the assumption of the model in mind, this comparison is within acceptable limits.

Finally, good agreement is also seen in the comparison of the load which causes first cracks in the top of the slab at the first pier to appear. A difference of 5.8% is shown in Table 10. Considering the visual observation of cracking in the slab does not give any quantitative information on the extent of cracking through the slab, the reported cracking load could have been "surface deep" or halfway through the slab depth. Therefore, this comparison is considered to be within acceptable limits.

4.3.2 Comparison of Two Termination Options

As with example bridge one, two termination options were analyzed in order to yield results acceptable to Ref. 2 and to provide a solution with more extensive damages. For continuous structures, the program will usually terminate when three layers of a concrete plate element are cracked (low termination option). A second computer analysis was also made which terminated when the maximum allowable crack width was exceeded (high termination option).

Table 11 presents a summary of the results from the two analyses. The first analysis already has some sizeable damages to the concrete slab, while the second analysis has extensive damages to the concrete deck. Unlike the first example bridge, the first analysis (low) appears to be a practical serviceability limit in the rating of bridges. Therefore, three cracked layers of one concrete plate element is recommended as the termination limit of the computer program. Higher loads than those predicted by this criterion are not recommended.

Another load-damage comparison can also be made. The dead load solutions for both analyses were identical in load. These results should be expected since the same dead loads were input into the program for the two analyses.

5. CONCLUSIONS

5.1 Conclusions

Based upon the comparisons between the experimental and the analytical results, the following observations and conclusions can be noted:

1. The overload structural response of steel girder-concrete slab highway bridges, in terms of stresses, deflections, and damages, can be predicted within acceptable limits by the detailed version of the modified program.
2. All four symmetry options were tested with satisfactory agreement in the comparisons made. For the simple span bridge, three symmetry options were analyzed with nearly identical results (less than 1% difference). The fourth symmetry option was tested for the continuous structure.
3. Present serviceability limits of the program may tend to be conservative for some bridges which terminate at 75% of the yield stress if residual stresses can be assumed negligible.

4. Bridges which terminate at three cracked layers within one plate element is probably an acceptable serviceability limit.
5. In continuous beam-slab bridge superstructures the first failure is the cracking of the concrete slab at the top surface in the negative moment region.
6. In simple span beam-slab bridge superstructures the first failure is the yielding of the steel girders in the bottom fibers either at the midspan or at the end of a coverplate.

5.2 Suggestions for Future Research

The observations and conclusions presented in the last section are those which were clearly evident in the examples studied as part of this research. It would be expected that further analytical results would confirm these conclusions. However, because the results already obtained come from only a limited number of tests, the following recommendations are made for future research:

1. An extensive parametric study on many different beam-slab bridge superstructures and loading patterns should be conducted using the detailed and simplified versions of the program. This study would more firmly establish overload

response characteristics and would allow for a comparison of results between the two program versions.

2. If possible, determine appropriate serviceability limits for frequent and infrequent overloads through experimental data, field observations, and analytical studies.
3. Compile an overload directory similar to the directory for concrete beam-concrete slab bridges (Ref. 20).
4. Investigate the variation of shear connector stiffness from full composite to partial composite to noncomposite. Verify the results of the results of the analytical method for partial composite and noncomposite bridges against experimental results.
5. Verify the simplified version of program BOVAS.

TABLE 1 EXAMPLE BRIDGE 1 - AASHTO 3B
SLAB REINFORCEMENT AND ORIENTATION

Bar Size	Spacing	Thickness	Centroid*	Angle
5	152 mm	1.312 mm	-10.5 mm	-90°
	6.0 in	0.0517 in	-0.413 in	
4	305 mm	0.4233 mm	3.81 mm	0°
	12.0 in	0.0167 in	0.150 in	
5	222 mm	0.9009 mm	32.7 mm	0°
	8.7 in	0.0355 in	1.288 in	
5	152 mm	1.312 mm	48.6 mm	-90°
	6.0 in	0.0517 in	1.913 in	

*Positive indicates below the slab mid-plane

TABLE 2 EXAMPLE BRIDGE 1 - AASHTO 3B

MATERIAL PROPERTIES

Material	Property	ACTUAL*		BOVAS**	
		(MPa)	(ksi)	(MPa)	(ksi)
Concrete	f'_c	39.58	5.74	39.58	5.74
Concrete	f_t	--	--	3.17	0.459
Concrete	E_c	35,852	5,200	30,098	4,365
Reinforcing Steel	σ_y	422	61.2	422	61.2
Reinforcing Steel	E_i	198,569	28,800	199,948	29,000
Girder Steel	σ_y, flange	242	35.1	248	36.0
Girder Steel	σ_y, web	275	39.9	290	42.0
Girder Steel	σ_y, cover-plate	268	38.9	290	42.0
Girder Steel	E_i	206,842	30,000	199,948	29,000

*These properties are taken from Ref. 17

**These properties were used in the analytical model-program BOVAS.

TABLE 3 EXAMPLE BRIDGE 2 - UNIVERSITY OF TENNESSEE BRIDGE 1

SLAB REINFORCEMENT AND ORIENTATION

Bar Size	Spacing	Thickness	Centroid*	Angle
5	140 mm	1.432 mm	-17.5 mm	-90°
	5.5 in	0.0564 in	-0.688 in	
5**	318 mm	0.630 mm	- 1.59 mm	0°
	12.5 in	0.0248 in	-0.063 in	
6**	319 mm	0.889 mm	- 1.59 mm	0°
	12.6 in	0.0350 in	-0.063 in	
5	203 mm	0.985 mm	39.7 mm	0°
	8.0 in	0.0389 in	1.563 in	
5	140 mm	1.432 mm	55.6 mm	-90°
	5.5 in	0.0564 in	2.188 in	

*Positive indicates below the slab mid-plane.

**These two reinforcement layers compose the top longitudinal steel reinforcement layer.

TABLE 4 EXAMPLE BRIDGE 2 - UNIVERSITY OF TENNESSEE BRIDGE 1

MATERIAL PROPERTIES

Material	Property	BOVAS* (MPa)	(ksi)
Concrete	f'_c	47.37	6.87
Concrete	f_t	3.38	0.490
Concrete	E_c	32,929	4,776
Reinforcing Steel	σ_y	275.8	40.0
Reinforcing Steel	E_i	199,948	29,000
Girder Steel	σ_y	289.6	42.0
Girder Steel	E_i	199,948	29,000

*These properties were used in the analytical model, program BOVAS.

TABLE 5 EXAMPLE BRIDGE 1 - AASHTO 3B

EXPERIMENTAL-ANALYTICAL COMPARISONS

		Experimental*	Analytical**
Load-Deflection Comparison			
75% of Yield Stress Load	(kN)	370.1	370.1
	(kips)	83.2	83.2
Max. Deflection at $\mathbb{C}_L$	(mm)	18.3	24.4
	(in)	0.72	0.96
Dead Load on Beam Solution			
Max. Stress at Midspan			
Exterior Girder (MPa)	(MPa)	101.4	94.5
	(ksi)	14.7	13.7
Interior Girder	(MPa)	90.3	87.6
	(ksi)	13.1	12.7
Dead Load on Structure Solution			
Max. Stress at End of Coverplate			
Exterior Girder	(MPa)	130.3	107.6
	(ksi)	18.9	15.6
Interior Girder	(MPa)	110.3	99.3
	(ksi)	16.0	14.4

TABLE 5 EXAMPLE BRIDGE 1 - AASHTO 3B

EXPERIMENTAL-ANALYTICAL COMPARISONS

		Experimental*	Analytical**
Max. Stress at Midspan			
Exterior Girder	(MPa)	113.8	100.7
	(ksi)	16.5	14.6
Interior Girder	(MPa)	96.5	93.1
	(ksi)	14.0	13.5

*The experimental results are taken from the text and figures of Ref. 18

**The results of the FULL symmetry analysis are used for this comparison.

TABLE 6 EXAMPLE BRIDGE 1 - AASHTO 3B

LOW TERMINATION SYMMETRY COMPARISONS (75% σ_y) - LOAD-DAMAGE

		Quarter*	Half-Transverse*	Full
Dead Load On Beam Load	(kN)	346.1	346.1	346.1
	(kips)	77.8	77.8	77.8
Dead Load on Structure Load	(kN)	17.8	17.8	17.8
	(kips)	4.0	4.0	4.0
Termination Load w/Impact	(kN)	369.6	370.1	370.1
	(kips)	83.1	83.2	83.2
Termination Load w/o Impact	(kN)	287.4	287.8	287.8
	(kips)	64.6	64.7	64.7
Max. Deflection at $\mathbb{C}_L$	(mm)	24.3	24.4	24.4
	(in)	0.958	0.959	0.960
Number of Yielded Layers		0	0	0
Number of Cracked Layers		0	0	0

*Quarter and half-transverse results are reported as if the symmetry was full in order to facilitate an easier comparison.

TABLE 7 EXAMPLE BRIDGE 1 - AASHTO 3B

LOW TERMINATION SYMMETRY COMPARISONS (75% σ_y) - MAXIMUM STRESSES*

		Quarter	Half-Transverse	Full
Dead Load on Beam Solution				
@ End of Coverplate				
Exterior Girder	(MPa)	101.4	101.4	101.4
	(ksi)	14.7	14.7	14.7
Interior Girder	(MPa)	93.1	93.1	93.1
	(ksi)	13.5	13.5	13.5
@ Midspan				
Exterior Girder	(MPa)	94.5	94.5	94.5
	(ksi)	13.7	13.7	13.7
Interior Girder	(MPa)	87.6	87.6	87.6
	(ksi)	12.7	12.7	12.7
Dead Load on Structure Solution				
@ End of Coverplate				
Exterior Girder	(MPa)	107.6	107.6	107.6
	(ksi)	15.6	15.6	15.6
Interior Girder	(MPa)	99.3	99.3	99.3
	(ksi)	14.4	14.4	14.4

TABLE 7 EXAMPLE BRIDGE 1 - AASHTO 3B (continued)

LOW TERMINATION SYMMETRY COMPARISONS (75% σ_y) - MAXIMUM STRESSES*

		Quarter	Half-Transverse	Full
@ Midspan				
Exterior Girder	(MPa)	100.7	100.7	100.7
	(ksi)	14.6	14.6	14.6
Interior Girder	(MPa)	93.1	93.1	93.1
	(ksi)	13.5	13.5	13.5
Overload Solution				
@ End of Coverplate				
Exterior Girder	(MPa)	195.8	195.8	195.8
	(ksi)	28.4	28.4	28.4
Interior Girder	(MPa)	188.2	188.2	187.5
	(ksi)	27.3	27.3	27.2
@ Midspan				
Exterior Girder	(MPa)	187.5	188.2	188.2
	(ksi)	27.2	27.3	27.3
Interior Girder	(MPa)	180.6	180.6	180.6
	(ksi)	26.2	26.2	26.2

*All stresses reported in this table are at the bottom fiber of the girder.

TABLE 8 EXAMPLE BRIDGE 1 - AASHTO 3B

LOW TERMINATION SYMMETRY COMPARISONS (MAX. CRACK WIDTH)

LOAD-DAMAGE

		Quarter*	Half-Transverse*	Full
Dead Load on Beam Load	(kN)	346.1	346.1	346.1
	(kips)	77.8	77.8	77.8
Dead Load on Structure Load	(kN)	17.8	17.8	17.8
	(kips)	4.0	4.0	4.0
Termination Load w/Impact	(kN)	1303.3	1306.9	1294.0
	(kips)	293.0	293.8	290.9
Termination Load w/o Impact	(kN)	1013.7	1016.4	1006.2
	(kips)	227.9	228.5	226.2
Max. Deflection at C_L	(mm)	242.2	246.0	236.9
	(in)	9.535	9.685	9.327
Number of Yielded Layers		180	180	179
Number of Cracked Layers		132	132	136

*Quarter and half-transverse results are reported as if the symmetry was full in order to facilitate an easier comparison.

TABLE 9 EXAMPLE BRIDGE 1 - AASHTO 3B

HIGH TERMINATION SYMMETRY COMPARISONS (MAX. CRACK WIDTH)

- MAXIMUM STRESSES

		Quarter	Half-Transverse	Full
Dead Load on Beam Solution*				
@ End of Coverplate				
Exterior Girder	(MPa)	101.4	101.4	101.4
	(ksi)	14.7	14.7	14.7
Interior Girder	(MPa)	93.1	93.1	93.1
	(ksi)	13.5	13.5	13.5
@ Midspan				
Exterior Girder	(MPa)	94.5	94.5	94.5
	(ksi)	13.7	13.7	13.7
Interior Girder	(MPa)	87.6	87.6	87.6
	(ksi)	12.7	12.7	12.7
Dead Load on Structure Solution*				
@ End of Coverplate				
Exterior Girder	(MPa)	107.6	107.6	107.6
	(ksi)	15.6	15.6	15.6
Interior Girder	(MPa)	99.3	99.3	99.3
	(ksi)	14.4	14.4	14.4

TABLE 9 EXAMPLE BRIDGE 1 - AASHTO 3B (continued)

HIGH TERMINATION SYMMETRY COMPARISONS (MAX. CRACK WIDTH)

- MAXIMUM STRESSES

		Quarter	Half-Transverse	Full
@ Midspan				
Exterior Girder	(MPa)	100.7	100.7	100.7
	(ksi)	14.6	14.6	14.6
Interior Girder	(MPa)	93.1	93.1	93.1
	(ksi)	13.5	13.5	13.5
Overload Solution**				
@ End of Coverplate				
Exterior Girder	(MPa)	375.1	380.6	369.6
	(ksi)	54.4	55.2	53.6
Interior Girder	(MPa)	375.8	378.5	376.5
	(ksi)	54.5	54.9	54.6
@ Midspan				
Exterior Girder	(MPa)	355.1	353.7	368.2
	(ksi)	51.5	51.3	53.4
Interior Girder	(MPa)	354.4	353.7	368.9
	(ksi)	51.4	51.3	53.5

*Reported stresses are for the bottom fiber of the girder.

**Rported stresses are in the web of the girder.

TABLE 10 EXAMPLE BRIDGE 2 - UNIVERSITY OF TENNESSEE BRIDGE 1

EXPERIMENTAL - ANALYTICAL COMPARISONS

		Experimental*	Analytical
Load-Deflection Comparisons			
Low Termination Load	(kN)	2041.7	2041.7
	(kips)	459.0	459.0
Deflection at Exterior Girder	(mm)	43.5	42.4
	(in)	1.71	1.67
Deflection at Centerline	(mm)	54.9	55.9
	(in)	2.16	2.20
High Termination Load	(kN)	3461.6	3461.6
	(kips)	778.2	778.2
Deflection at Exterior Girder	(mm)	76.2	71.4
	(in)	3.00	2.81
Deflection at Centerline	(mm)	109.7	107.2
	(in.)	4.32	4.22
Load Comparisons			
First Yield Load	(kN)	2757.9	3100.0
	(kips)	620.0	696.9
First Cracks @ Pier 1	(kN)	2891.3	2722.3
	(kips)	650.0	612.0

*The experimental results are taken from the text and figures of Ref. 6.

TABLE 11 EXAMPLE BRIDGE 2 - UNIVERSITY OF TENNESSEE BRIDGE 1

LOAD-DAMAGE COMPARISONS

		Low*	High**
Dead Load on Beam Load	(kN)	5252.9	5252.9
	(kips)	1180.9	1180.9
Dead Load on Structure Load	(kN)	89.0	89.0
	(kips)	20.0	20.0
Termination Load w/Impact	(kN)	2041.7	3461.6
	(kips)	459.0	778.2
Termination Load w/o Impact	(kN)	1641.4	2782.8
	(kips)	369.0	625.6
Max. Deflection at $\mathbb{C}_L$	(mm)	55.9	107.2
	(in)	2.20	4.22
Number of Yielded Layers		0	6
Number of Cracked Layers		23	92

*Low corresponds to a termination of 3 cracked layers in one element.

**High corresponds to a termination of maximum crack width exceeded.

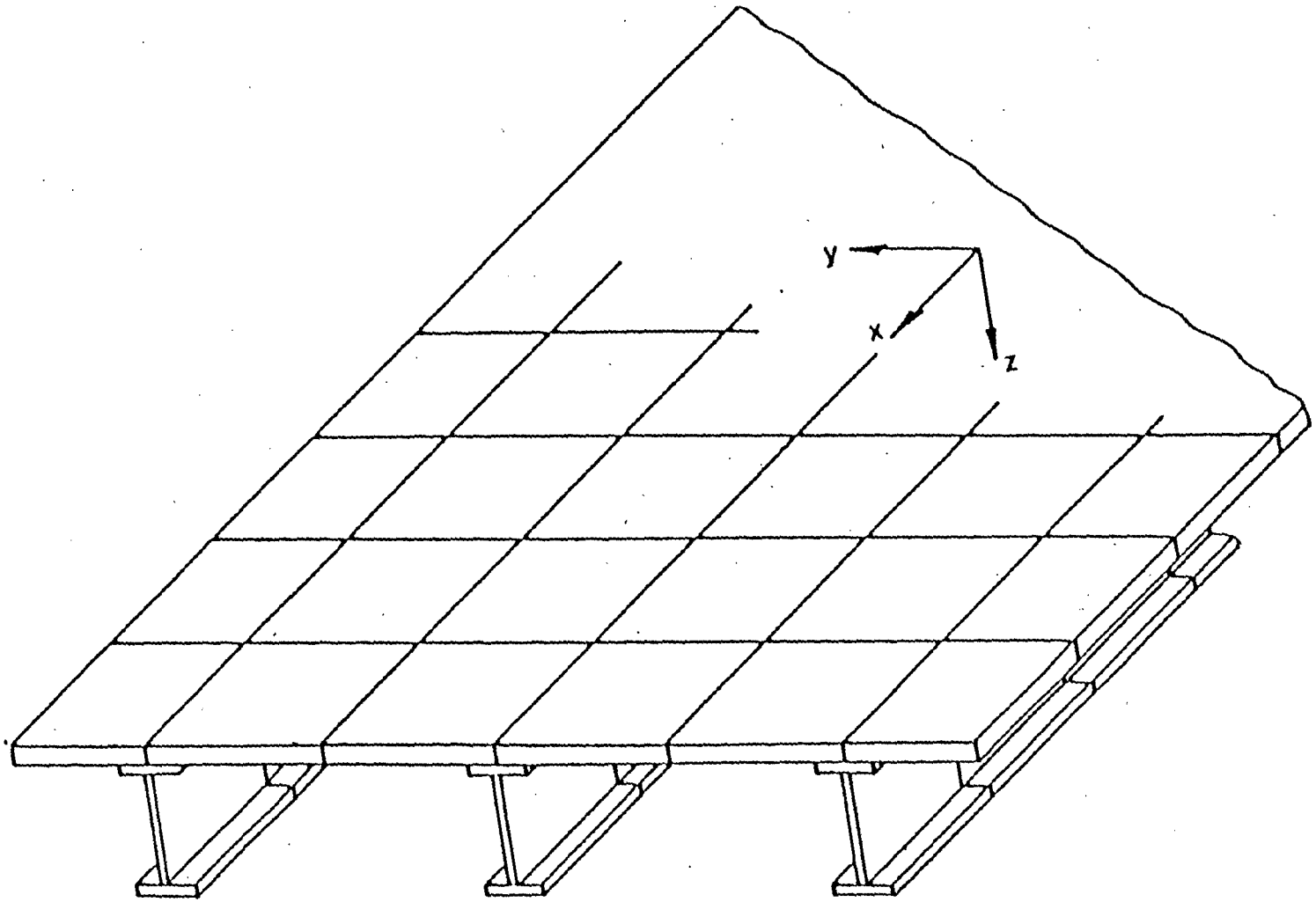

Fig. 1 Typical Slab-Girder Highway Bridge Finite Element Discretization

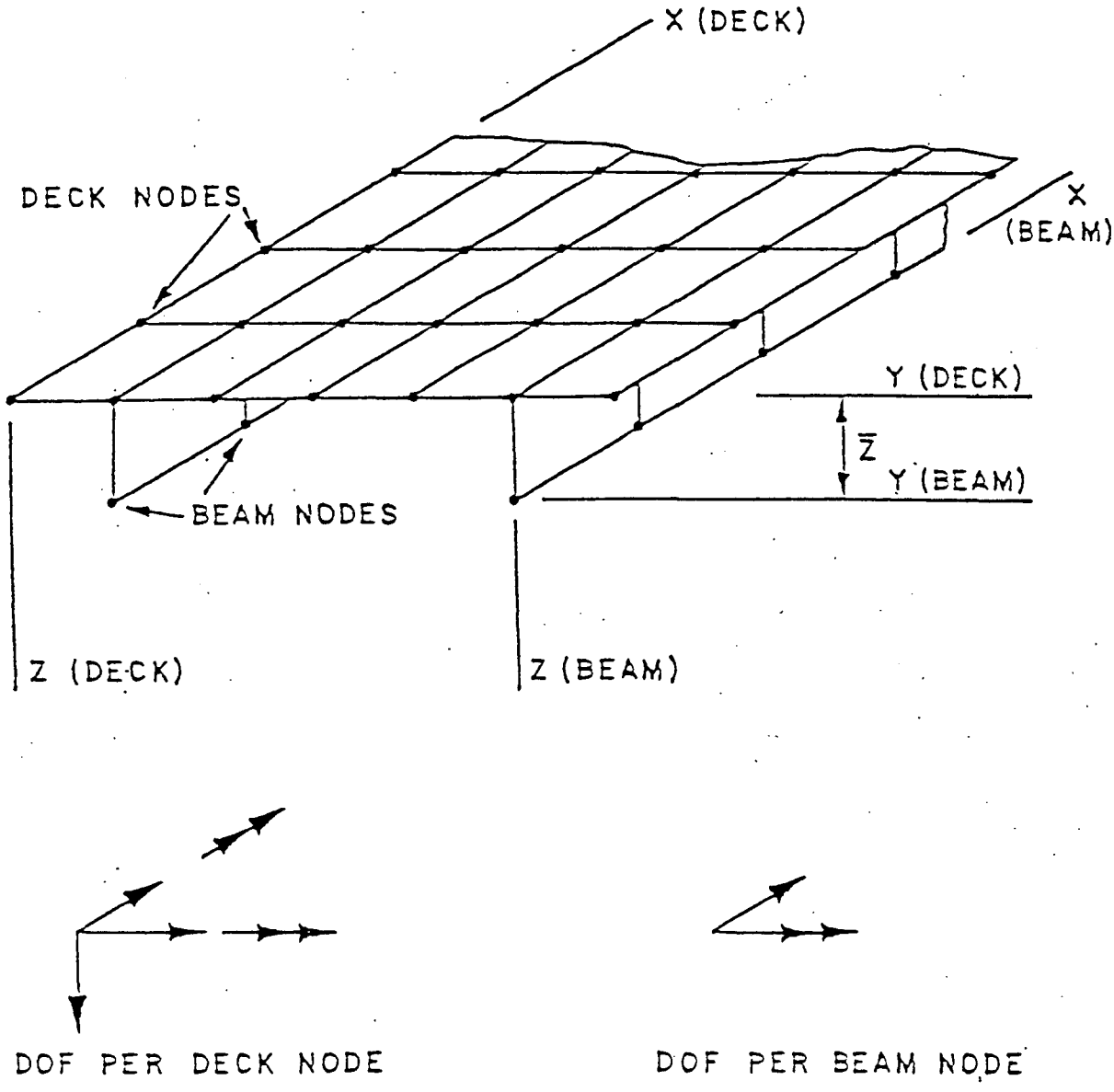

Fig. 2 Beam and Slab Node Point Arrangement

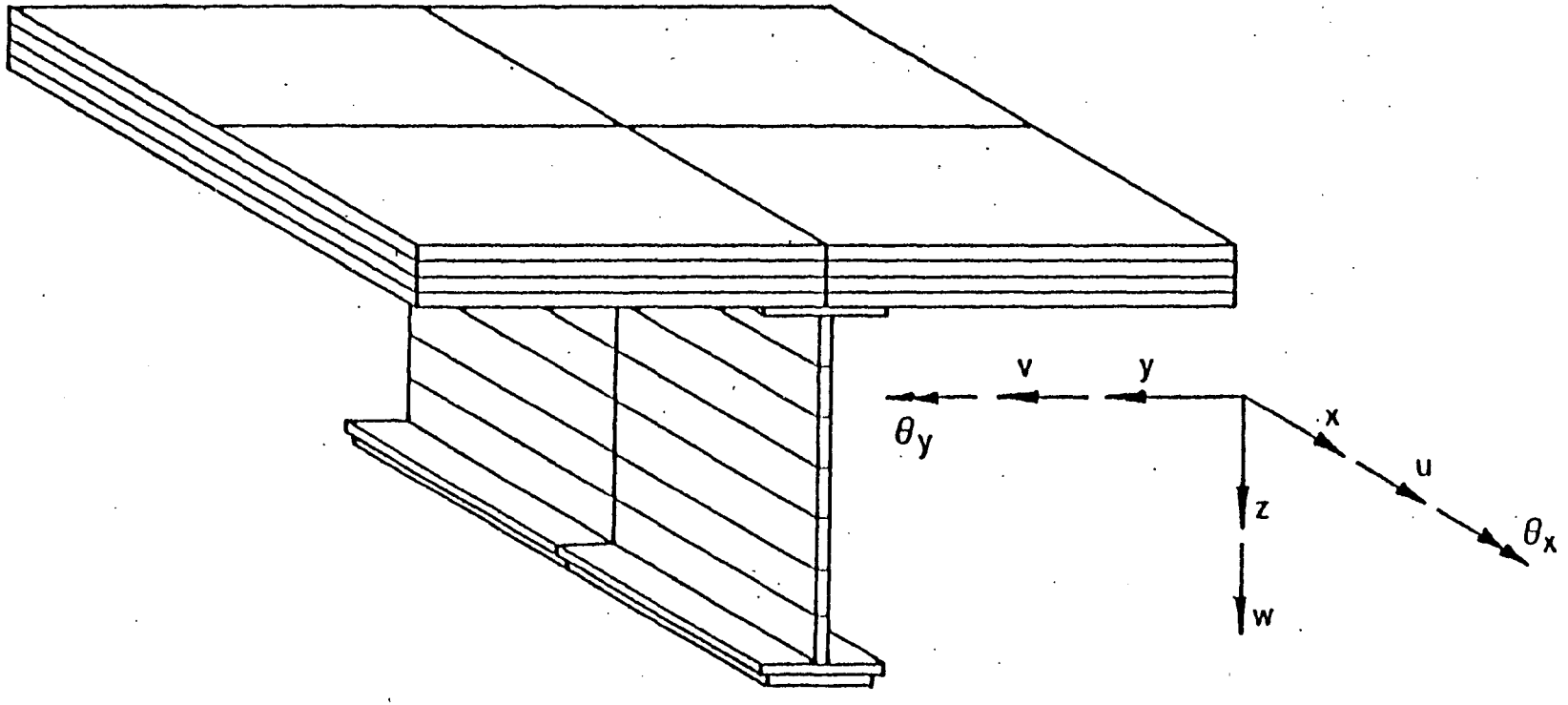

Fig. 3 Slab and Girder Layering

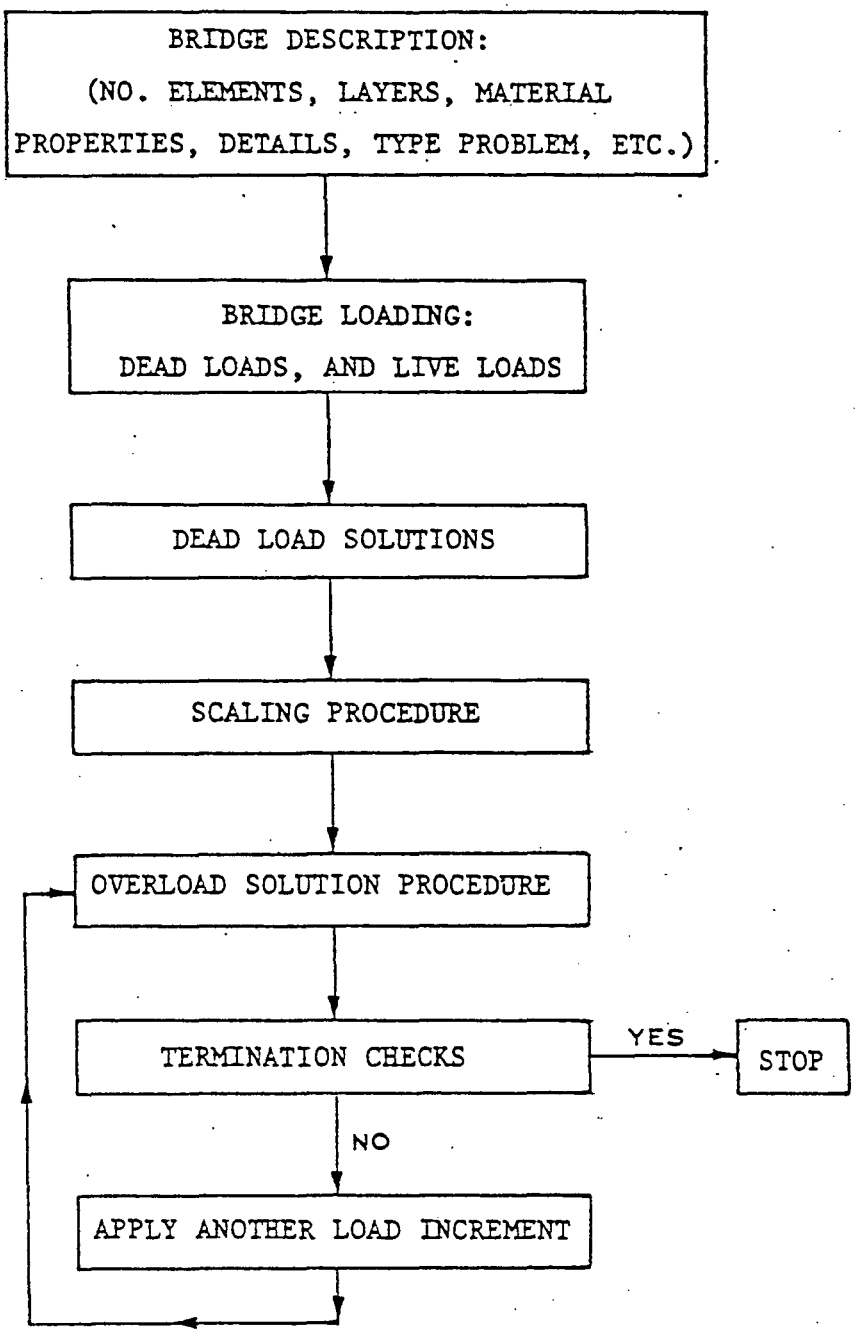

Fig. 4 Flow Chart BOVAS Solution Scheme

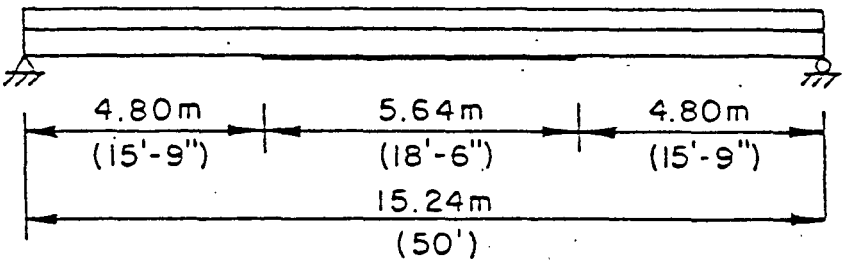

Fig. 5 Example No. 1 - AASHTO Bridge 3B - Elevation

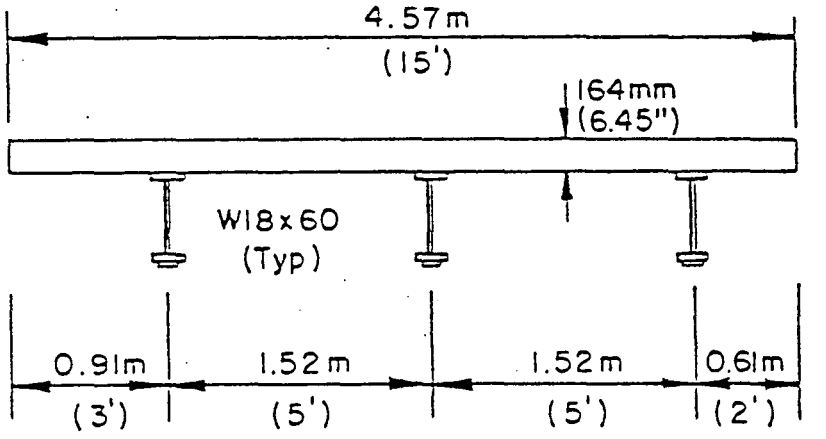

Fig. 6 Example No. 1 - AASHTO Bridge 3B - Cross-Section

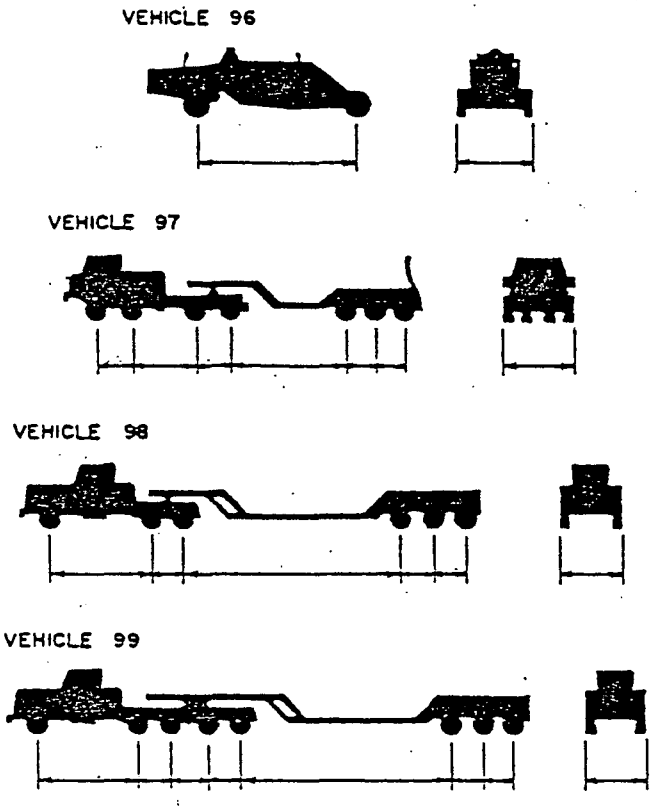

Fig. 7 Overloaded Test Vehicles - Example No. 1

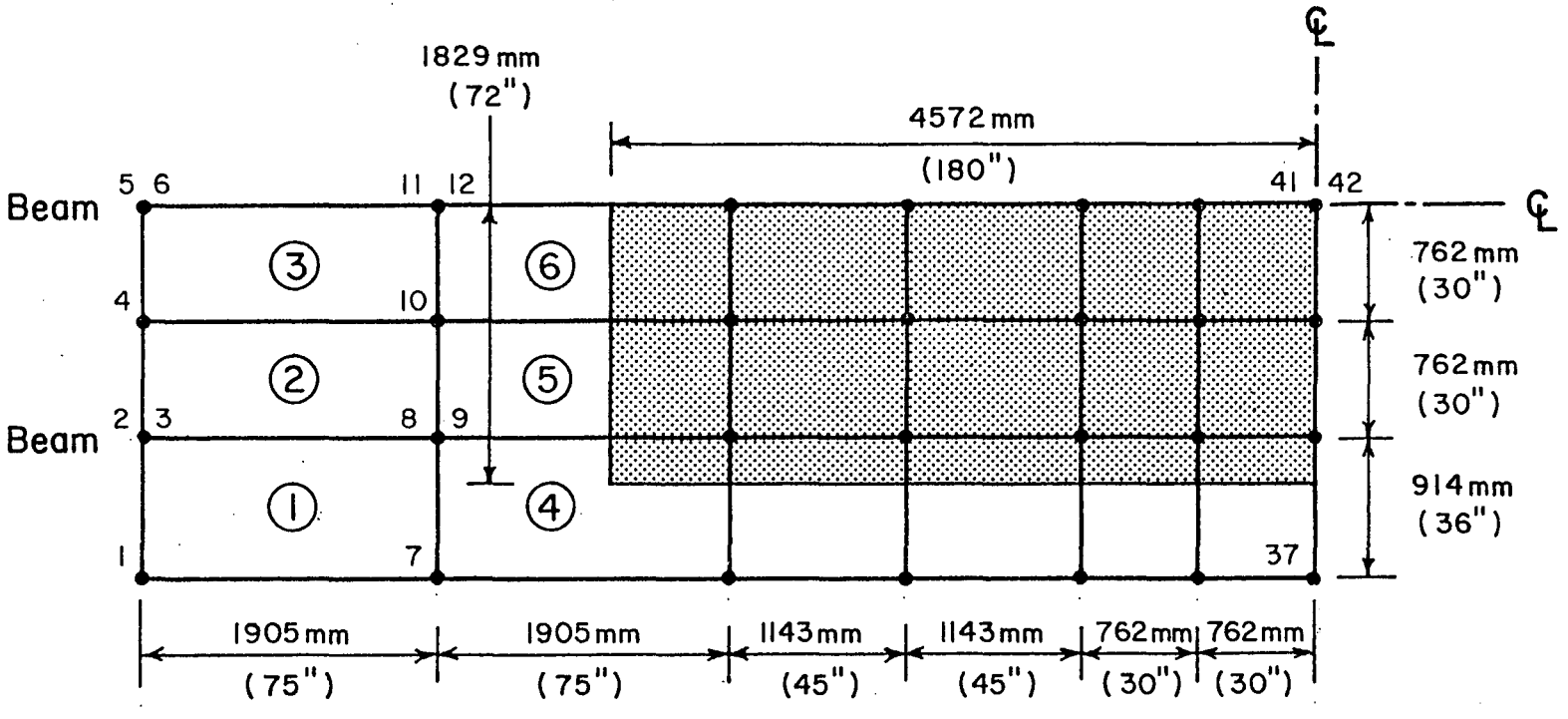

Fig. 8 Example No. 1 - AASHTO Bridge 3B - Finite Element Discretization - Quarter Symmetry

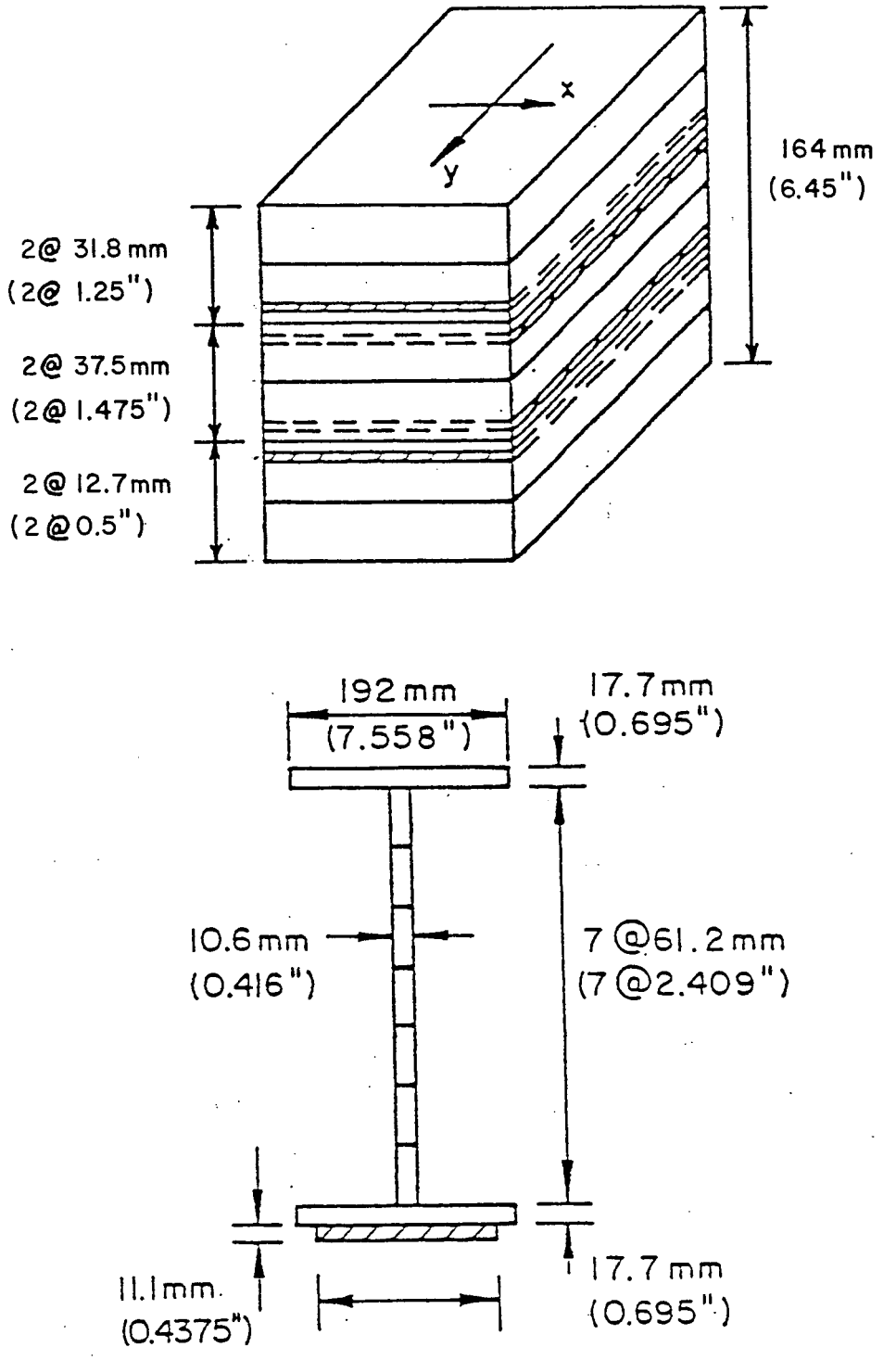

Fig. 9 Example No. 1 - Slab and Beam Layering

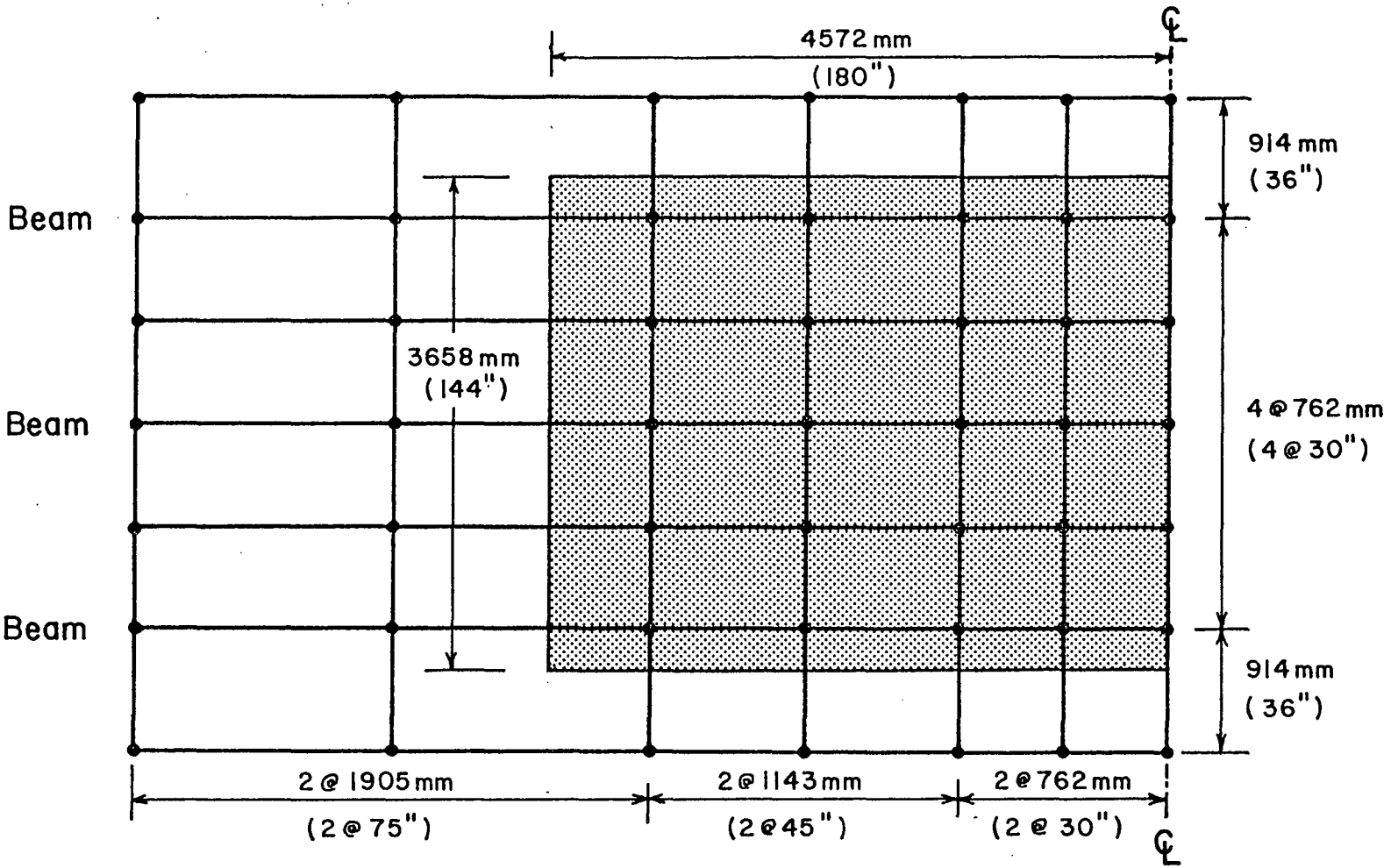

Fig. 10 Example No. 1 - AASHTO Bridge 3B - Finite Element Discretization - Half-Transverse Symmetry

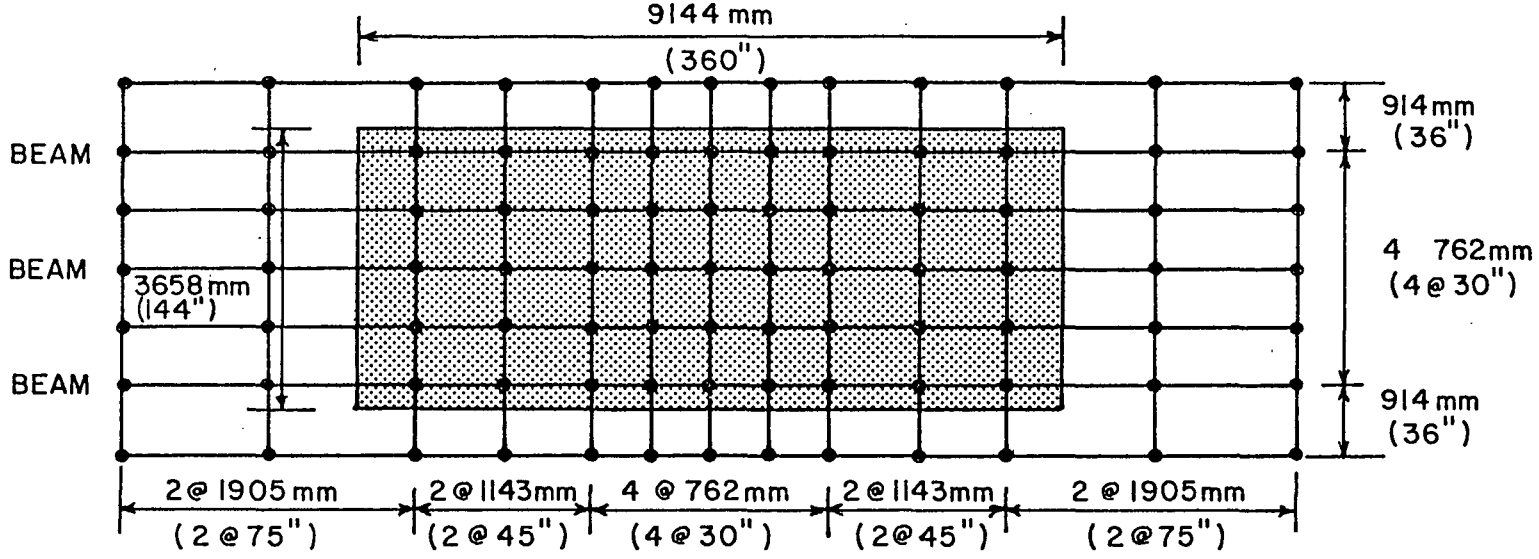

Fig. 11 Example No. 1 - AASHTO Bridge 3B - Finite Element Discretization - Full Symmetry

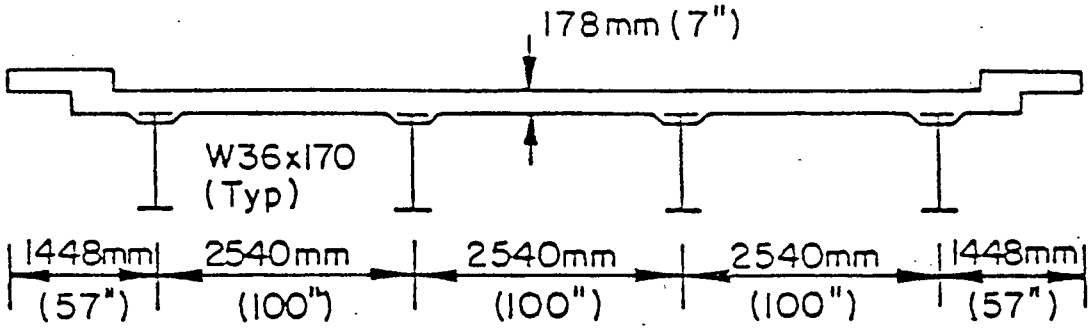

(a) Example No. 2 Actual Cross Section

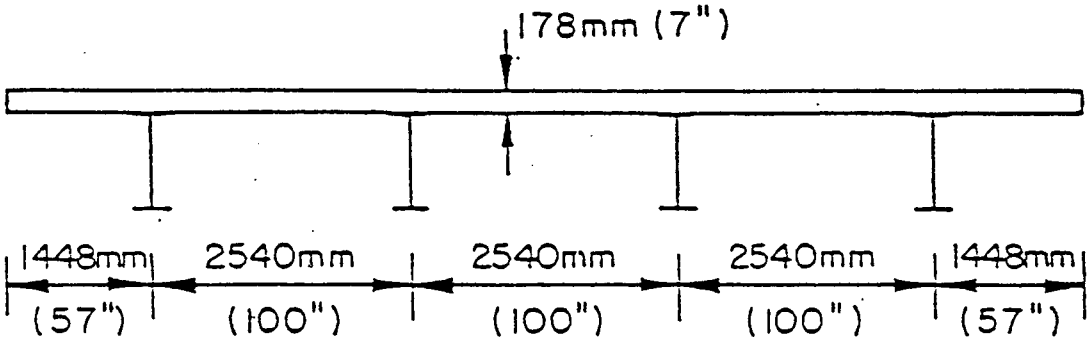

(b) Example No. 2 Idealized Cross Section

Fig. 12 Example No. 2 - Actual Cross-Section and Idealized Cross Section

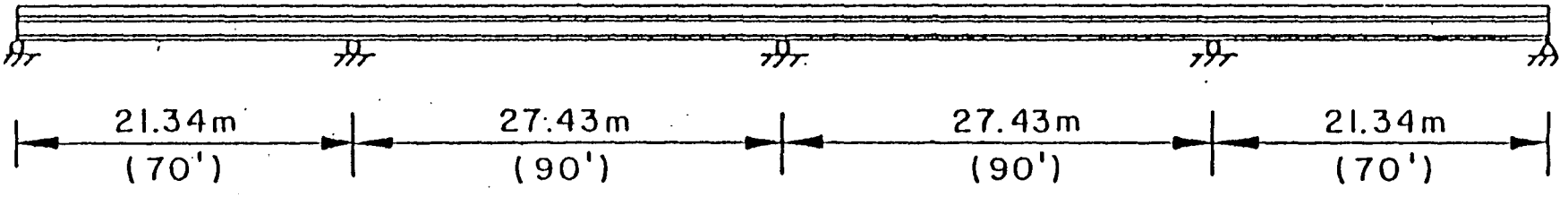

(a) Example No. 2 Elevation

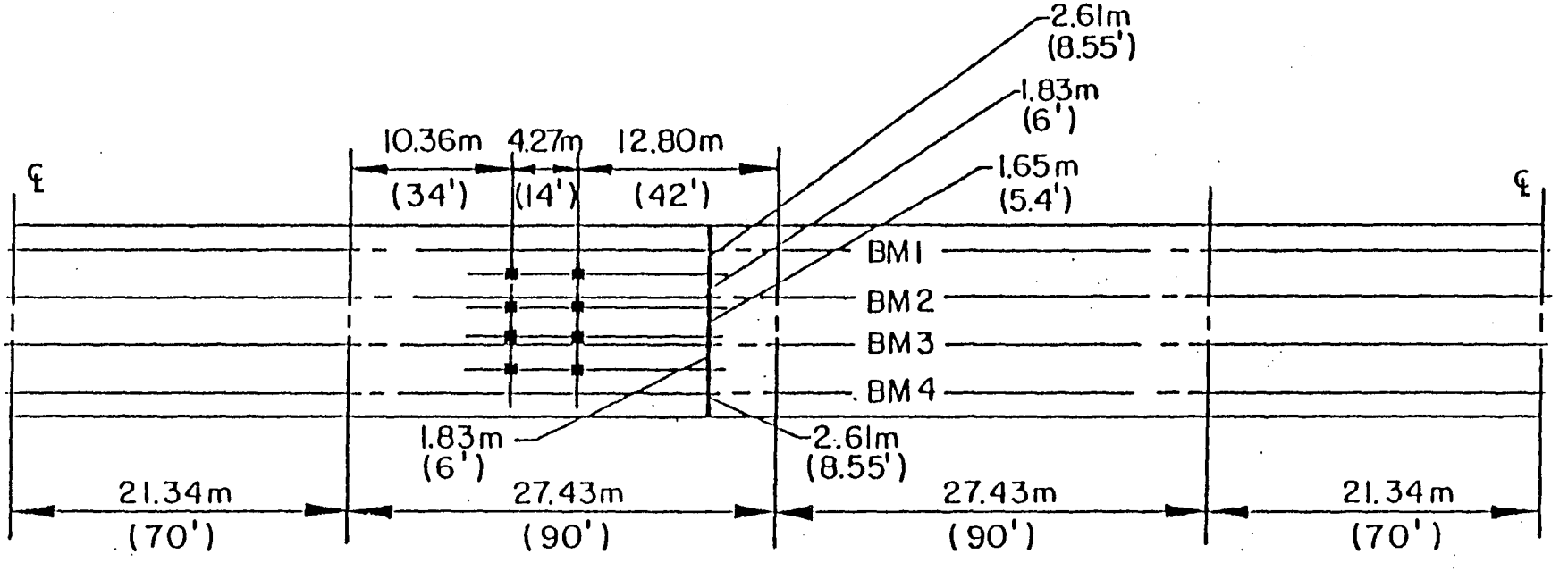

(b) Example No. 2 Plan and Loading

Fig. 13 Example No. 2 - Finite Element Discretization

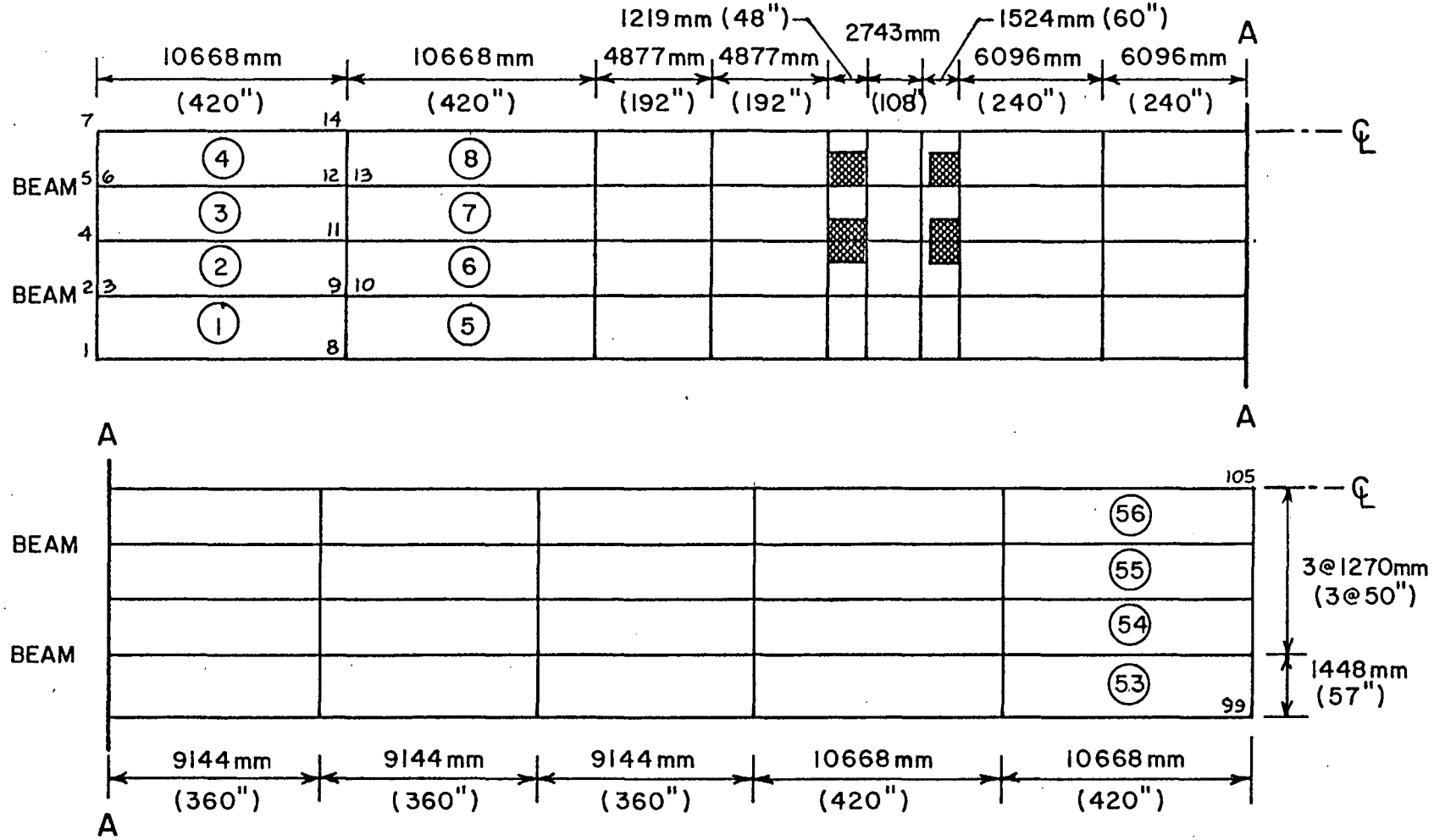

Fig. 14 Example No. 2 - Finite Element Discretization

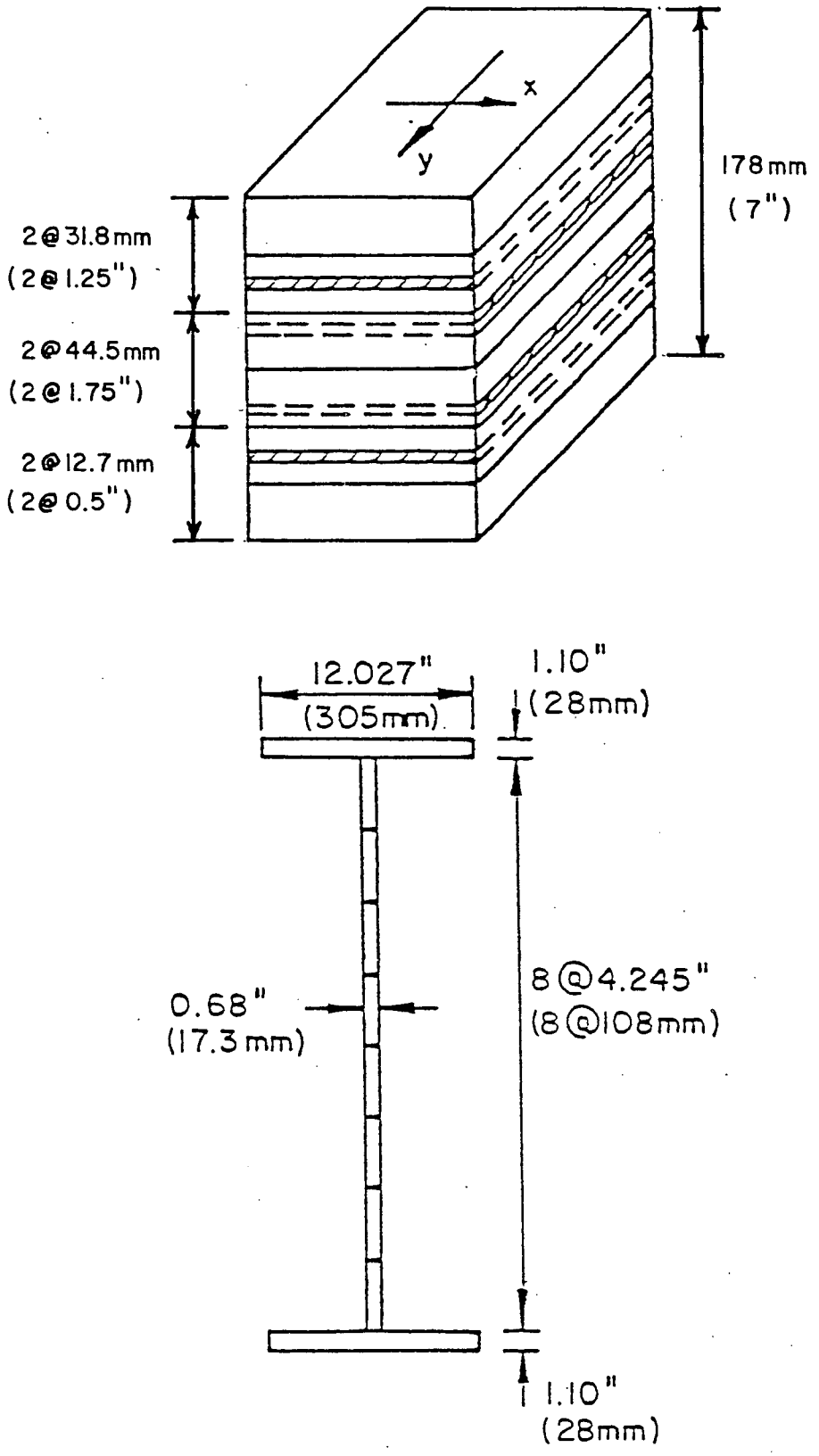

Fig. 15 Example No. 2 - Slab and Beam Layering

REFERENCES

1. Adini, A. and Clough, R. W.
   ANALYSIS OF PLATE BENDING BY THE FINITE ELEMENT METHOD, Report submitted to the National Science Foundation, Grant G7337, University of California, Berkeley, California, 1960.

2. American Association of State Highway and Transportation Officials
   MANUAL FOR MAINTENANCE INSPECTION OF BRIDGES, Washington, D. C., 1978.

3. American Association of State Highway and Transportation Officials,
   STANDARD SPECIFICATIONS FOR HIGHWAY BRIDGES, Washington, D. C., 1977.

4. Baldwin, J. W., Jr., Henry, J. R., and Sweeney, C. M.
   STUDY OF COMPOSITE BRIDGE STRINGERS, PHASE II, University of Missouri, Columbia, Missouri, May 1965.

5. Barnard, P. R.
   RESEARCHES INTO THE COMPLETE STRESS-STRAIN CURVE FOR CONCRETE, Magazine of Concrete Research, Vol. 16, No. 49, December 1964.

6. Burdette, E. G. and Goodpasture, D. W.
   FINAL REPORT ON FULL SCALE BRIDGE TESTING - AN EVALUATION ON BRIDGE DESIGN CRITERIA, University of Tennessee, 1971.

7. Clough, R. W.
   THE FINITE ELEMENT METHOD IN STRUCTURAL MECHANICS, Chapter 7 of Stress Analysis, edited by O. C. Zienkiewicz and G. S. Hollister, John Wiley and Sons, New York, New York, 1965.

8. Dia, P. K., Thiruvengadam, T. R., and Siess, C. P.
   INELASTIC ANALYSIS OF COMPOSITE BEAMS, Engineering Extension Series No. 15, Proc. ASCE Specialty Conference on Steel Structures, University of Missouri, Columbia, June 8-12, 1970.

9. Fu, C. C., Colville, J. and Heins, C. P.
INELASTIC ANALYSIS OF CONTINUOUS COMPOSITE HIGHWAY BRIDGES, Civil Engineering Report No. 62, University of Maryland, College Park, Maryland, June 1976.

10. Hall, J. C. and Kostem, C. N.
INELASTIC ANALYSIS OF STEEL MULTI-GIRDER HIGHWAY BRIDGES, Fritz Engineering Laboratory Report No. 435.1, Lehigh University, Bethlehem, Pennsylvania, August 1980.

11. Hall, J. C. and Kostem, C. N.
FURTHER STUDIES ON THE INELASTIC OVERLOAD RESPONSE OF STEEL MULTI-GIRDER BRIDGES, Fritz Engineering Laboratory Report No. 435.2, Lehigh University, Bethlehem, Pennsylvania, March 1981.

12. Hall, J. C. and Kostem, C. N.
INELASTIC OVERLOAD ANALYSIS OF CONTINUOUS STEEL MULTI-GIRDER HIGHWAY BRIDGES BY THE FINITE ELEMENT METHOD, Fritz Engineering Laboratory Report No. 432.6, Lehigh University, Bethlehem, Pennsylvania, June 1981.

13. Hand, F. R., Pecknold, D. A., and Schnobrich, W. C.
A LAYERED FINITE ELEMENT NONLINEAR ANALYSIS OF REINFORCED CONCRETE PLATES AND SHELLS, Civil Engineering Studies, Structural Research Series No. 389, University of Illinois, Urbana, Illinois, August 1972.

14. Hand, F. R., Pecknold, D. A., and Schnobrich, W. C.
NONLINEAR LAYERED ANALYSIS OF RC PLATES AND SHELLS, Journal of the Structural Division, ASCE, Vol. 99, No. ST7, July 1973.

15. Heishman, C. A. and Kostem, C. N.
USER'S MANUAL FOR THE DETAILED VERSION OF PROGRAM BOVAS, Fritz Engineering Laboratory Report No. 435.4, Lehigh University, Bethlehem, Pennsylvania, September 1982.

16. Heishman, C. A. and Kostem, C. N.
USER'S MANUAL FOR THE SIMPLIFIED VERSION OF PROGRAM BOVAS, Fritz Engineering Laboratory Report No. 435.5, Lehigh University, Bethlehem, Pennsylvania, September 1982.

17. Highway Research Board
THE AASHO ROAD TEST, Report 2, MATERIALS AND CONSTRUCTION, Special Report 61B, 1962.

18. Highway Research Board
THE AASHO ROAD TEST, Report 4, BRIDGE RESEARCH, Special Report 61D, 1962.

19. Johnston, B. G., Editor
GUIDE TO STABILITY DESIGN CRITERIA FOR METAL STRUCTURES, 3rd Edition, John Wiley & Sons, New York, New York, 1976.

20. Kostem C. N.
OVERLOADING OF HIGHWAY BRIDGES A PARAMETRIC STUDY, Fritz Engineering Laboratory Report No. 378B.7, Lehigh University, Bethlehem, Pennsylvania, August 1976.

21. Kostem, C. N.
OVERLOADING BEHAVIOR OF BEAM-SLAB TYPE HIGHWAY BRIDGES, Fritz Engineering Laboratory Report No. 378B.8, Lehigh University, Bethlehem, Pennsylvania, July 1977.

22. Kulicki, J. M. and Kostem, C. N.
THE INELASTIC ANALYSIS OF REINFORCED AND PRESTRESSED CONCRETE BEAMS, Fritz Engineering Laboratory Report No. 378B.1, Lehigh University, Bethlehem, Pennsylvania, November 1972.

23. Kulicki, J. M. and Kostem, C. N.
FURTHER STUDIES ON THE NONLINEAR FINITE ELEMENT ANALYSIS OF BEAMS, Fritz Engineering Laboratory Report No. 378A.5, Lehigh University, Bethlehem, Pennsylvania, April 1973.

24. Kulicki, J. M. and Kostem, C. N.
THE INELASTIC ANALYSIS OF PRESTRESSED AND REINFORCED CONCRETE BRIDGE BEAMS BY THE FINITE ELEMENT METHOD, Fritz Engineering Laboratory Report No. 378A.6, Lehigh University, Bethlehem, Pennsylvania, September 1973.

25. Kupfer, H., Hilsdorf, H. K. and Rusch, H.
BEHAVIOR OF CONCRETE UNDER BIAXIAL STRESSES, Journal of the American Concrete Institute, Vol. 66, No. 8, August 1969.

26. Lin, C. S.
NONLINEAR ANALYSIS OF REINFORCED CONCRETE SLABS AND SHELLS, Ph.D. Dissertation, University of California, Berkeley, California, September 1972.

27. Liu, T. C.
STRESS-STRAIN RESPONSE AND FRACTURE OF CONCRETE IN BIAXIAL COMPRESSION, Ph.D. Dissertation, Structural Engineering Department, Cornell University, Ithaca, New York, 1971.

28. Neilissen, L. J. M.
BIAXIAL TESTING OF NORMAL CONCRETE, HERON, Vol. 18, No. 1, 1972, Stevin-Laboratory of the Department of Civil Engineering of the Technological University and Institute TNO for Building Materials and Building Structures, Delft, The Netherlands.

29. Newmark, N. M.
A DISTRIBUTION PROCEDURE FOR THE ANALYSIS OF SLABS CONTINUOUS OVER FLEXIBLE BEAMS, University of Illinois Engineering Experiment Station Bulletin No. 304, University of Illinois, Urbana, 1938.

30. Pennsylvania Department of Transportation
STANDARDS FOR BRIDGE DESIGN, Series BD-100, Harrisburg, Pennsylvania, May 1976.

31. Peterson, W. S., Kostem, C. N. and Kulicki, J. M.
THE INELASTIC ANALYTIS OF REINFORCED CONCRETE SLABS, Fritz Engineering Laboratory Report No. 378B.3, Lehigh University, Bethlehem, Pennsylvania, May 1974.

32. Peterson, W. S., Kostem, C. N. and Kulicki, J. M.
DISCUSSION OF "FULL RANGE ANALYSIS OF ECCENTRICALLY STIFFENED PLATES", by A. N. Wegmuller, Journal of the Structural Division, ASCE, Vol. 100, ST9, September 1974.

33. Peterson, W. S. and Kostem, C. N.
THE INELASTIC ANALYSIS OF BEAM-SLAB HIGHWAY BRIDGE SUPERSTRUCTURES, Fritz Engineering Laboratory Report No. 378B.5, Lehigh University, Bethlehem, Pennsylvania, March 1975.

34. Peterson, W. S. and Kostem, C. N.
THE INELASTIC ANALYSIS OF BEAM-SLAB BRIDGES, Fritz Engineering Laboratory Report No. 400.20, Lehigh University, Bethlehem, Pennsylvania, July 1975.

35. Ramberg, W. and Osgood, W. R.
DESCRIPTION OF STRESS-STRAIN CURVES BY THREE PARAMETERS, NACA, TN 902, July 1943.

36. Siess, C. P., Viest, I. M. amd Newmark, N. M.
STUDIES OF SLAB AND BEAM HIGHWAY BRIDGES, PART III - SMALL SCALE TESTS OF SHEAR CONNECTORS AND COMPOSITE I-BEAMS, University of Illinois Engineering Bulletin No. 396, University of Illinois, Urbana, 1952.

37. Tumminelli, S. C. and Kostem, C. N.
FINITE ELEMENT ANALYSIS FOR ELASTIC ANALYSIS OF COMPOSITE BEAMS AND BRIDGES, Fritz Engineering Laboratory Report No. 432.3, Lehigh University, Bethlehem, Pennsylvania, March 1978.

38. Wegmuller, A. W. and Kostem, C. N.
ELASTIC-PLASTIC ANALYSIS OF PLATES, Proceedings of the IASS Symposium on Shell Structures and Climatic Influences, pp. 379-386, Calgary, Canada, July 1972.

39. Wegmuller, A. W. and Kostem, C. N.
FINITE ELEMENT ANALYSIS OF PLATES AND ECCENTRICALLY STIFFENED PLATES, Fritz Engineering Laboratory Report No. 378A.3, Lehigh University, Bethlehem, Pennsylvania, February 1973.

40. Wegmuller, A. W. and Kostem, C. N.
FINITE ELEMENT ANALYSIS OF ELASTIC-PLASTIC PLATES AND ECCENTRICALLY STIFFENED PLATES, Fritz Engineering Laboratory Report No. 378A.4, Lehigh University, Bethlehem, Pennsylvania, February 1973.

41. Whang, B.
ELASTO-PLASTIC ORTHOTROPIC PLATES AND SHELLS, Proceedings of the Symposium on Application of Finite Element Methods in Civil Engineering, Vanderbilt University, Nashville, Tennessee, November 1969.

42. Wu, Y. C.
ANALYSIS OF CONTINUOUS COMPOSITE BEAMS, Ph.D. Dissertation, Lehigh University, Bethlehem, Pennsylvania, December 1970.

43. Yam, L. C. P. and Chapman, J. C.
THE INELASTIC BEHAVIOR OF SIMPLY SUPPORTED COMPOSITE BEAMS OF STEEL AND CONCRETE, Proceedings of the Institution of Civil Engineering, London, December 1968.